Optical Control of Ca^{2+}-Mediated Morphological Response in Glial Cells with Visible Light Using a Photocaged Kainoid

Zhenlin Tian,[#,†] Mitra Sadat Tabatabaee,[#,‡] Simon Edelmann,[†] Julien Gibon[§] and Frederic Menard[*,†,‡]

[†] Department of Chemistry, [‡] Department of Biochemistry & Molecular Biology, [§] Department of Biology, I.K. Barber School of Sciences, The University of British Columbia, Kelowna, BC, Canada V1V 1V7

Supporting Information Placehold

ABSTRACT A chemical probe (DECM-PhKA) was developed to study filopodia extension in glial cells with spatio-temporal control. Irradiating DECM-PhKA with blue light releases the neuroactive agonist phenylkainic acid with a half-lifetime of 61 seconds. The effect of rapid uncaging was demonstrated in U118-MG astrocyte cells. The agonist is released locally with high precision using an optic fiber to trigger calcium influx that leads to filopodia extension in the targeted cells. This chemical probe provides a new tool to study the contribution of kainate receptors in transduction of external signals at the single cell level using a physiologically compatible wavelength.

In the brain, ionotropic glutamate receptors (iGluRs) expressed in neurons are the primary mediators of excitatory neurotransmission.[1] They are also found in glia where their role remains undefined.[2,3] iGluRs are membrane-bound ion channels that open upon glutamate binding to allow an influx of cations such as calcium.[4] iGluRs are categorized into three subgroups based on their sensitivity to agonists: α-amino-3-hydroxy-5-methyl-4-isoxazole propionic acid (AMPA), *N*-methyl-D-aspartic acid (NMDA), and kainic acid (KA).[5] Their expression levels, localization and distribution vary widely according to the type of cells, environment, developmental stage, age, stimulation, etc.[2,6,7] The three subgroups respond to glutamate, making it a major challenge to distinguish the exact role of each in neurological diseases.[8,9] Pioneering work by Trauner and coworkers has made available chemical tools to selectively control and study AMPA[10,11] and NMDA[12] receptors. However, the role of KA receptors (KARs) in neurophysiology is still understudied due to the lack of molecular tools for their selective activation.[13-16]

Optically controllable molecules offer attractive means to study ion channels, as they enable one to manipulate a protein's activity with spatio-temporal resolution.[17,18] While optogenetics is a powerful biological approach to control neuronal activity with light, this technique requires genetic manipulation for each organism investigated.[19-22] Photopharmacological tools offer a complementary approach to control physiological events.[23] One type of such molecular tools are photocaged compounds, where a biologically active compound is protected with a photochromic group that is cleaved upon light irradiation.[24,25] To conduct meaningful time-dependent studies of dynamic processes (e.g., events at synapses), the uncaging process must be rapid, and at a wavelength that is not harmful to cells.

Herein, we report a photocaged kainoid for the optical control of kainate receptors using blue visible light (Figure 1). The caged kainoid **1** (DECM-PhKA), bears a photocleavable carbamate on its pyrrolidine nitrogen. This secondary amine is essential to the binding of kainic acid analogs to the KAR protein, thus, protecting it makes **1** biologically inactive.[26] As cage moiety, we selected a 7-*N*,*N*-diethylaminocoumarin (DECM) carbamate because it can be cleaved by blue light sources equipped on most modern microscopes to release phenylkainic acid (PhKA, **2**) as active KAR agonist. Consequently, DECM-PhKA should act as a "turn-on" probe to study KAR activity in living cells.

Activation of glutamate receptors with photocaged ligands was first demonstrated elegantly by Ellis- Davies with 4-methoxy-7-nitroinodolinyl caged glutamate

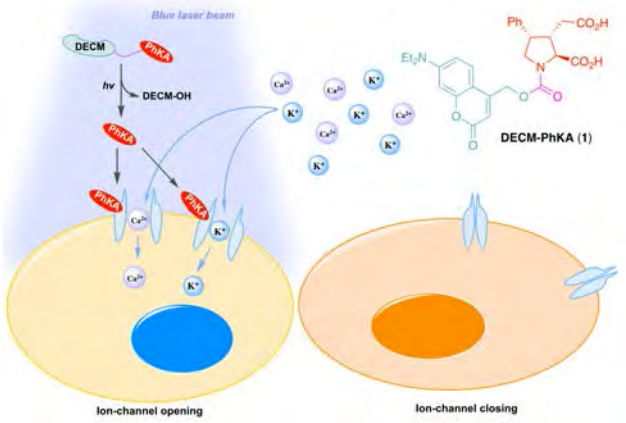

Figure 1. Proposed blue-light releasable agonist DECM-PhKA and the mechanism of ion influx triggered by light irradiation.

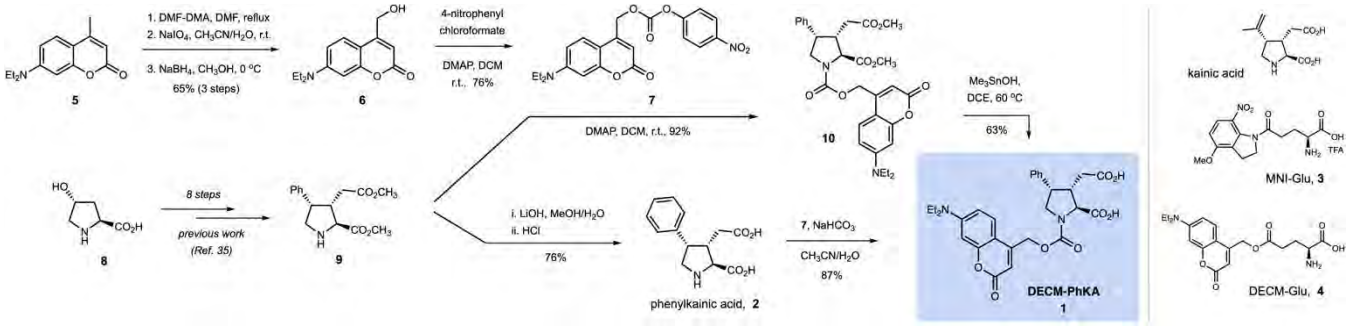

Scheme 1. Synthesis of DECM-PhKA

(MNI-Glu, **3**, Scheme 1).[27,28] However, MNI-Glu is uncaged with UV light (lethal wavelength for cells) which limits its use to study long term phenomena in cells or tissue. Alternatively, the DECM group was used as a cage for glutamate because it is excited with light in the visible region and it has a higher quantum yield (DECM-Glu, **4**).[29,30]

While DECM-Glu is useful in biological context, it releases glutamate which activates several receptors indiscriminately: ionotropic (GluA's, GluN's, GluK's) and metabolotropic glutamate receptors (mGluR1-8), thereby preventing selective investigations of their individual roles.

With the goal of creating a KAR-specific activator, we combined a DECM cage with one of the most potent KAR ligand synthetically accessible on scale: PhKA (> 50-fold more active than glutamate for KAR).[31-33] We describe below the synthesis, characterization, and application of the novel probe—DECM-PhKA (**1**) to activate KARs upon blue light irradiation.

Synthesis of Photocaged Agonists. The synthesis of DECM-PhKA capitalizes on the advanced pyrrolidine intermediate **9** we reported previously.[35] The coumaryl cage precursor **7** was prepared in four steps (Scheme 1). 4-Methyl-7-*N,N*-diethyl amino-coumarin (**5**) was condensed with methylformamide dimethylacetal to afford enamine **5a**, which was then oxidized with sodium periodate to yield aldehyde **5b** (Scheme S1). Reduction of the aldehyde with sodium borohydride provided alcohol **6**. This oxidation/reduction sequence was adopted instead of a direct selenium dioxide allylic oxidation due to its higher reproducibility and lower cost on large scale.[34] Alcohol **6** was then coupled with 4-nitrophenyl chloroformate to afford the unsymmetrical carbonate **7** as caging reagent. The 4-nitrophenyl group was chosen because of its enhanced reactivity and nucleofugacity over the unstable coumaryl alkoxyde.

Diester pyrrolidine **9** was reacted with the unsymmetrical DECM carbonate **7** to give fully protected phenylkainoid **10**. All attempts to hydrolyze diester **10** selectively under basic conditions also cleaved the DECM carbamate group (e.g., LiOH aq./CH_3OH). Using milder conditions (trimethyltin hydroxide)[36] provided the desired caged phenylkainic acid **1**, but the product also contained residual tin that not could be removed by chromatography. Alternative methods were explored since even traces of tin raise high cytotoxicity concerns in live cell experiments.[37] The successful sequence involved hydrolyzing pyrrolidine **9** to PhKA **2**, then directly reacting the free aminodiacid with the cage reagent carbonate **7**. This alternative route circumvented using heavy metal reagents and afforded the desired caged compound DECM-PhKA (**1**) in an acceptable yield.

In parallel to the synthesis of DECM-PhKA, we also prepared MNI-Glu (**3**) and DECM-Glu (**4**) as positive controls to examine how **1** compares with existing photocaged iGluR agonists. MNI-Glu was synthesized from 4-methoxyindole and glutamic acid in six steps with a 34% overall yield according to a reported sequence (Scheme S2).[38] DECM-Glu was synthesized from Boc-Glu-OtBu and alcohol **6** in two steps with a 75% overall yield using optimized reactions (Scheme S3).[28,29,39]

Photolysis Characterization. Photolysis reactions with the caged agonists **1**, **3** and **4** were performed with blue light in aqueous solutions to assess their reactivity under physiological conditions and were characterized by ^{1}H NMR spectroscopy in D_2O. The photocleavage conditions were optimized with DECM-Glu ester (**4**) at room temperature, with either a photoreactor equipped with a 445 nm blue LED light source (100 W), or a 465 nm LED array (33 W, Figures S3-S8). Photolysis of the DECM ester group was much faster when irradiated with a 445 nm (Figure S7) than a 465 nm (Figure S6) light source due to a better overlap of the emission and the absorption of DECM-Glu (Figure S1). More specifically, at 445 nm, full cleavage was observed after 140 seconds; and at

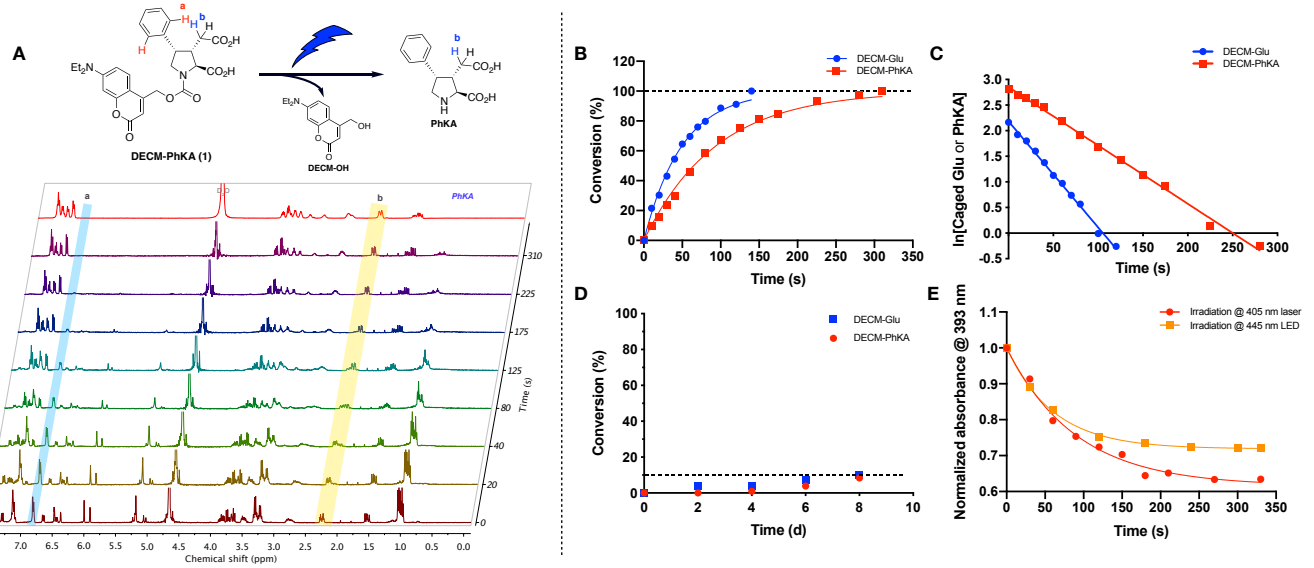

Figure 2. Photolysis kinetics of the caged agonists. (A) Overlaid ^{1}H NMR spectra of the photolysis process DECM-PhKA (**1**) as function of time irradiated with blue light (445 nm). Top spectrum in A is pure phenylkainic acid (**2**) for reference (red trace). The depth axis shows time intervals of ^{1}H NMR spectra acquisition. (B, C) DECM-Glu and DECM-PhKA were cleaved with a 445 nm LED lamp. (D) Stability of DECM-Glu and DECM-PhKA under natural light in the lab. (E) Photolysis of DECM-PhKA with a 445 nm LED light or a 405 nm laser; the process was monitored by UV-Vis spectral analysis.

465 nm, even after 16 minutes of irradiation only 80% conversion was observed (Figure S8).

With the DECM-PhKA carbamate (**1**), the agonist PhKA was completely uncaged within 300 seconds at 445 nm (Figure 2A). In the reaction, diagnostic peaks of the CH_2 *alpha* to the carboxylic acid of PhKA (peak *b*) shift from 2.29 ppm to 2.20 ppm. Similarly, the *ortho* hydrogens on the C4 phenyl group of DECM-PhKA shift from 6.84 ppm to 7.03 ppm. The integration of both sets was averaged to quantify the photolysis.

Kinetic experiments confirmed that releasing PhKA with visible light irradiation in aqueous solution is rapid and efficient. The photolysis rates were calculated from the analysis of sequential ^{1}H NMR spectra (Figure 2B-C). The ester group of DECM-Glu was cleaved at a faster rate than the carbamate of DECM-PhKA: the half-life time for DECM-Glu is 33.4 s and that of DECM-PhKA is 60.8 s (Table 1). While both compounds carry the same coumaryl chromophore, the difference in uncaging rate can be rationalized by the carbamate group in **1** undergoing a slower photolysis the ester in **4**. A similar trend was reported with MNI-caged glutamate derivatives.[42]

The uncaging of DECM-PhKA with laser irradiation at 405 nm was also evaluated as this wavelength is commonly found on most confocal microscopes (Figure 2E). The photolysis rate with a focused 405 nm laser beam was 1.5 times faster than with whole sample irradiation with a LED collimated light source (Table 1). This more efficient photocleavage could partially be caused by a greater spectral overlap of the laser (405 nm) emission with the absorption of DECM-PhKA (Figure S1).

Table 1. Photochemical Properties of Caged Glu and PhKA

Compounds	λ_{max} *(nm)*	*K* (s^{-1})	$T_{1/2}$ *(s)*
MNI-Glu	339	–	–
DECM-Glu	390	1.66×10^{-3} [a]	417[a]
		2.07×10^{-2} [b]	33.4[b]
DECM-PhKA	393	1.14×10^{-2} [b]	60.8[b]
		1.66×10^{-2} [c]	41.7[c]

a. Irradiated by 465 nm LED lamp; b. Irradiated by 445 nm LED lamp; c. Irradiated by 405 nm laser.

As expected, MNI-Glu showed virtually no photolysis when irradiated with a 445 nm blue LED light source over 5 minutes (Figures S1 and S2A). In contrast, both DECM-Glu and DECM-PhKA were completely photocleaved after five minutes under the same conditions (Figures S2B-C). No uncaging occurred when DECM-PhKA was irradiated at 445 nm in anhydrous DMSO, confirming that a stoichiometric amount of water is necessary to the photolytic process (Figure S2D).

The photolysis kinetics of the DECM carbamate follow a pseudo first-order relationship (Figure 2B). The photolysis mechanism is proposed to involve the initial dissociation of [CM-A] to the excited ion pair $[CM^+ \bullet A^-]^*$ in a first-order manner (Figure S4).[40,41] The resulting CM^+ and A^- then react with H_2O to yield CM-OH and AH products (where AH is Glu or PhKA). Without water, $[CM^+ \bullet A^-]^*$ can relax and recombine to the ground state of CMA.

Stability of DECM-PhKA. The thermal stability of caged agonists **1** and **4** in solution under normal lab light was also investigated (Figure 2D). When samples of **1** and **4** were left to stand at room temperature while exposed to ambient lab lights, less than ~10% of DECM-PhKA was cleaved after 8 days (Figure 2D). Thus, the stability of the caged compounds is excellent for manipulations in biological experiments (typically lasting a few hours at most), with the new carbamate **1** being slightly more stable than ester **4**.

Optical Control of Filopodia Extension in Glial Cells. We designed DECM-PhKA to investigate whether kainate receptors can induce the extension of cellular processes in living glial cells.[43-45] In a tripartite synapse, astrocytes extend filopodia, seeking to contact neuronal dendritic spines to contribute to synapse formation,[46,47] but the exact mechanism of this morphological response is still undefined, mostly due to a lack of proper research tools.[48,49] Cultured astrocytes are known to extend filopodia upon glutamate stimulation that is associated with an intracellular calcium rise,[50] and early studies have

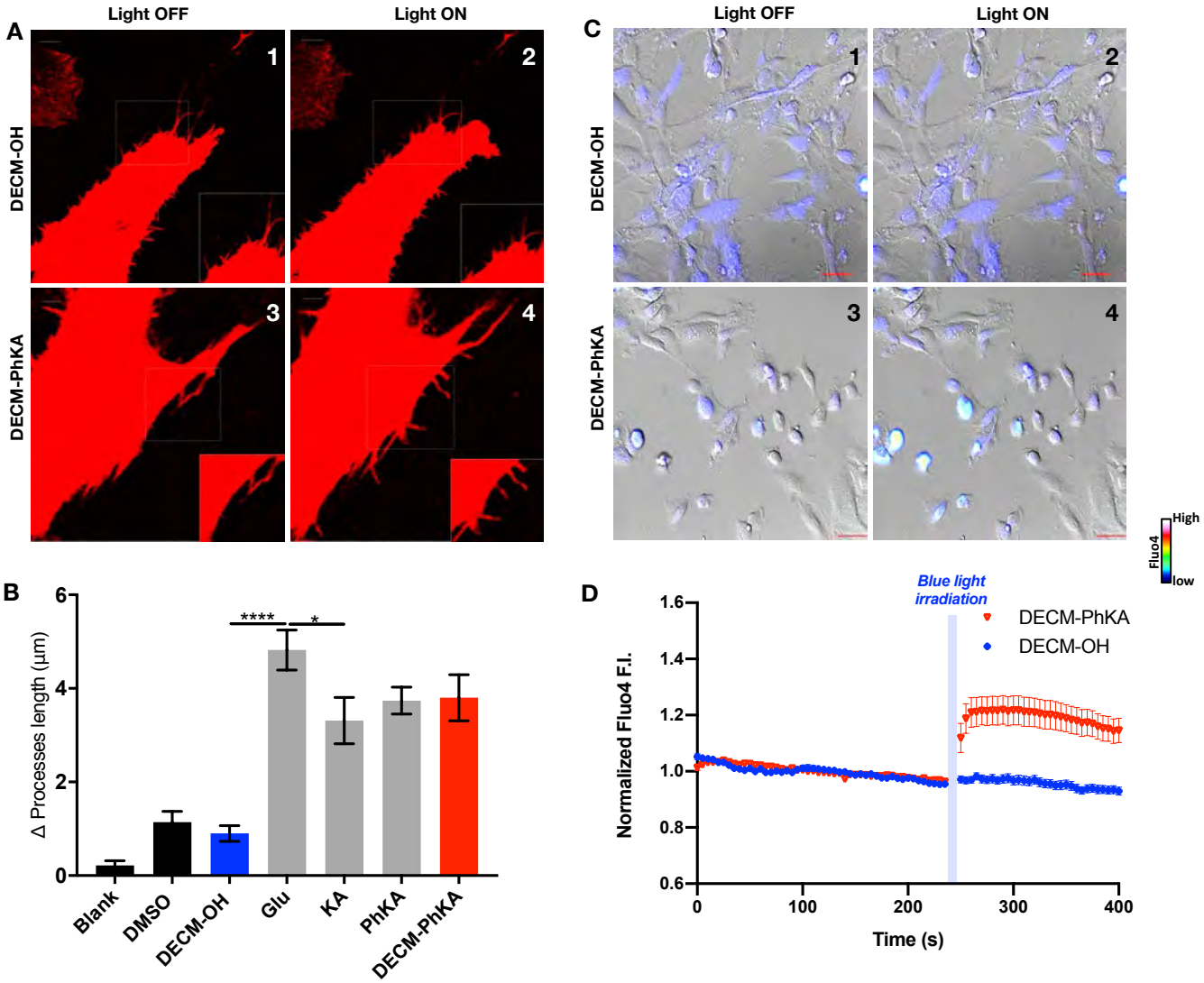

Figure 3. Photocleavage of DECM-PhKA promotes filopodia extension and increases intracellular calcium in model astrocytes. (**A**) Representative confocal micrographs of U118-MG astrocytoma cells treated with 2 mM DECM-OH and DECM-PhKA (in 0.01% DMSO) before and after exposure to 405 nm light. 60X objective lens, scale bar is 10 μM. (**B**) Cells extend their processes significantly in response to 100 μM solutions of glutamate, KA, PhKA, or DECM-PhKA + light (n = 5 independent experiments). Results are presented as mean ± SEM, *p <0.05, ****p < 0.0001 (One-way ANOVA followed by Tukey's multiple comparison test). (**C**) Representative fluorescent micrographs of U118-MG astrocytoma cells, pretreated with Fluo4-AM, upon irradiation of light to EDCM-OH and DECM-PhKA in 0.01% DMSO. 20X objective lens; scale bar is 100 μM. (**D**) Normalized Fluo4-AM fluorescence in the presence of 2 mM of DECM-PhKA or DECM-OH in U118-MG cells before and after light exposure (405 nm, via an optic fiber) (n = 133 cells for DECM and n = 100 cells for DECM-PhKA), results are presented as mean ± SEM.

shown that AMPA and KA trigger the same response.[51] While the role of AMPA receptors and mGluRs in astrocytes has been studied inconclusively,[43,52] no study has been reported on the function of kainate receptors.

Glutamate stimulation of astrocytoma U118-MG cells (model cell line for astrocytes) confirmed that they undergo the same morphological changes as astrocytes (Figures 3B and S9). Exposing the cells to a 100 μM glutamate solution caused rapid filopodia protrusion (measured over 20 minutes), and is consistent with observations reported in cultured cortical astrocytes.[51]

Photo-release of the caged compound DECM-PhKA (**1**) triggered rapid process extension in U118-MG cells upon a single *10-second illumination* with 405 nm blue light delivered *at the observed cell* using an fiber-optic (Figure 3A-B). Uncaging DECM-PhKA caused the extension of cellular processes similar to the whole-bath perfusion of a PhKA solution (3.58 ± 0.01 μm and 3.52 ± 0.01 μm, respectively, Figure 3B). We observed that PhKA caused slightly higher processes extension than that of KA (3.09 ± 0.01, Figure S9). The effect of pure glutamate was more pronounced than both KA and PhKA (4.60 ± 0.01), which may be due to the activation of additional glutamate receptors beside GluKs. Finally, control experiments showed that none of the DMSO vehicle, the caged DECM-PhKA, or the DECM-OH byproduct cause significant filopodia extension.

As further evidence that DECM-PhKA acts as a turn-on probe for iGluR channels, the photo-uncaging induced significant Ca^{2+} flux in cells as measured with the Fluo4-AM dye (Figure 3C-D). The glutamate-induced morphological response in astrocytes is known to be associated with an intracellular calcium flux required for cytoskeletal rearrangement in filopodia extension.[50] Accordingly, when U118 cells were pre-treated with the calcium sensor Fluo4-AM and DECM-PhKA, a 10-second irradiation with blue light induced a significant increase in fluorescence corresponding to Ca^{2+} chelation by Fluo4 (Figure 3C-D). Control experiments with DECM-OH did not show a change above background calcium levels within cells.

In conclusion, DECM-PhKA (**1**) is a novel molecular tool that can be used to activate glutamate receptors sensitive to kainic acid in living cells using visible light pulses. Uncaging kinetic experiments confirmed the rapid release of the agonist upon blue light illumination, yet the probe is stable to ambient light. DECM-PhKA can be used with a light source common to most modern imaging platforms, e.g., 405 nm laser. Measuring the morphological response in astrocytic model cells demonstrated that a 10-second light pulse with DECM-PhKA is sufficient to induce the protrusion of filopodia, which correlates with the associated intracellular Ca^{2+} flux. Illumination of a single cell is possible by using a fiber-optic. We anticipate that the precise control of GluK protein activation with probe **1** will enable the systematic investigations of the role of this glutamate receptor subtype in health and disease.

ASSOCIATED CONTENT

Supporting Information

Spectroscopic data for all compounds, 1D and 2D spectra of ^{1}H and ^{13}C NMR analyses. The Supporting Information is available free of charge on the ACS Publications website.

AUTHOR INFORMATION

Corresponding Author

* E-mail: frederic.menard@ubc.ca

Author Contributions

# ZT and MT contributed equally to this work.

ZT conducted the synthesis of probes and kinetic study, MT carried out the biological experiments, S.E. synthesized precursors of phenyl kainic acid, JG conducted and analyzed the calcium imaging experiments. ZT, MT and FM wrote the manuscript and prepared the figures.

Notes

The authors declare no competing financial interest.

ACKNOWLEDGMENTS

The work was carried out with the support by the Natural Science and Engineering Research Council of Canada (NSERC), the John R. Evans Leaders Fund from the Canadian Fund for Innovation (CFI-JELF), and the University of British Columbia. ZT and MT gratefully acknowledge UBC for University Graduate Fellowships and a Dean's Thesis Fellowship. We thank Dr. Paul Shipley for NMR support and Dr. Andis Klegeris for providing the cell lines. We are grateful to Dr. Vojtech Kapras for generous support with photoreactors.

REFERENCES

(1) Traynelis, S. F.; Wollmuth, L. P.; McBain, C. J.; Menniti, F. S.; Vance, K. M.; Ogden, K. K.; Hansen, K. B.; Yuan, H.; Myers, S. J.; Dingledine, R.; Sibley, D. *Pharmacol Rev.* **2010**, 62 (3), 405.
(2) Seifert, G.; Steinhäuser, C. *Prog. Brain. Res.* **2001**, 132, 287.
(3) Gallo, V.; Ghiani, C. A. *Trends Pharmacol. Sci.* **2000**, 21 (7), 252.
(4) Contractor, A.; Heinemann, S. F. *Sci. Signal.* **2002**, 2002 (156), re14.
(5) Armstrong, N.; Sun, Y.; Chen, G.-Q.; Gouaux, E. *Nature* **1998**, 395 (6705), 913.
(6) Oberheim, N. A.; Wang, X.; Goldman, S.; Nedergaard, M. *Trends Neurosci.* **2006**, 29 (10), 547.
(7) Nishida, H.; Okabe, S. *J. Neurosci.* **2007**, 27 (2), 331.
(8) Lemoine, D.; Jiang, R.; Taly, A.; Chataigneau, T.; Specht, A.; Grutter, T. *Chem. Rev.* **2012**, 112 (12), 6285.
(9) Traynelis, S. F.; Wollmuth, L. P.; McBain, C. J.; Menniti, F. S.; Vance, K. M.; Ogden, K. K.; Hansen, K. B.; Yuan, H.; Myers, S. J.; Dingledine, R.; Sibley, D. *Pharmacol. Rev.* **2010**, 62 (3), 405.
(10) Barber, D. M.; Liu, S.-A.; Gottschling, K.; Sumser, M.; Hollmann, M.; Trauner, D. *Chem. Sci.* **2017**, 8 (1), 611.
(11) Stawski, P.; Sumser, M.; Trauner, D. *Angew.Chem. Int. Ed.* **2012**, 51 (23), 5748.
(12) Laprell, L.; Repak, E.; Franckevicius, V.; Hartrampf, F.; Terhag, J.; Hollmann, M.; Sumser, M.; Rebola, N.; DiGregorio, D. A.; Trauner, D. *Nature Comm.* **2015**, 6 (1), 8076.

(13) Matute, C. *CNS Neurosci. Ther.* **2010**, 17 (6), 661.
(14) Jane, D. E.; Lodge, D.; Collingridge, G. L. *Neuropharmacol.* **2009**, 56 (1), 90.
(15) Lerma, J. *Nat. Rev. Neurosci.* **2003**, 4 (6), 481.
(16) Lerma, J.; Marques, J. M. *Neuron* **2013**, 80 (2), 292.
(17) Broichhagen, J.; Frank, J. A.; Trauner, D. *Acc. Chem. Res.* **2015**, 48 (7), 1947.
(18) Hüll, K.; Morstein, J.; Trauner, D. *Chem. Rev.* **2018**, 118 (21), 10710.
(19) Berndt, A.; Lee, S. Y.; Ramakrishnan, C.; Deisseroth, K. *Science* **2014**, 344 (6182), 420.
(20) Deisseroth, K.; Hegemann, P. *Science* **2017**, 357 (6356).
(21) Zhang, F.; Li-Ping, W.; Boyden, E. S. *Nat. Methods* **2006**, 3(10), 785.
(22) Pama, E. A. C.; Colzato, L. S.; Hommel, B. *Front. Psychol.* **2013**, 4, 610.
(23) Leippe, P.; Leman, J. K.; Trauner, D. *Biochemistry* 2017, 56 (39), 5214.
(24) Marvin, J. S.; Borghuis, B. G.; Tian, L.; Cichon, J.; Harnett, M. T.; Akerboom, J.; Gordus, A.; Renninger, S. L.; Chen, T.-W.; Bargmann, C. I.; Orger, M. B.; Schreiter, E. R.; Demb, J. B.; Gan, W.-B.; Hires, S. A.; Looger, L. L. *Nat. Methods* **2013**, 10 (2), 162.
(25) Palma-Cerda, F.; Auger, C.; Crawford, D. J.; Hodgson, A. C. C.; Reynolds, S. J.; Cowell, J. K.; Swift, K. A. D.; Cais, O.; Vyklicky, L.; Corrie, J. E. T.; Ogden, D. *Neuropharmacol.* **2012**, 63 (4), 624.
(26) Tian, Z.; Clark, B. L. M.; Menard, F. *ACS Chem. Neurosci.* **2019**, 10 (10), 4190.
(27) Matsuzaki, M.; Ellis-Davies, G. C. R.; Nemoto, T.; Miyashita, Y.; Iino, M.; Kasai, H. *Nat. Neurosci.* **2001**, 4 (11), 1086.
(28) Papageorgiou, G.; Ogden, D.; Kelly, G.; Corrie, J. E. T. *Photochem. Photobiol. Sci.* **2005**, 4 (11), 887.
(29) Vishakha R Shembekar; Yongli Chen; Barry K Carpenter, A.; George P Hess. *Biochemistry* **2005**, 44 (19), 7107.
(30) Olson, J. P.; Kwon, H.-B.; Takasaki, K. T.; Chiu, C. Q.; Higley, M. J.; Sabatini, B. L.; Ellis-Davies, G. C. R. *J. Am. Chem. Soc.* **2013**, 135 (16), 5954.
(31) Hashimoto, K.; Shirahama H.*Tetrahedron Lett.* **1991**, 32 (23), 2625.
(32) Jack E Baldwin; Andrew M Fryer, A.; Pritchard, G. J. *J. Org. Chem.* **2001**, 66 (8), 2588.
(33) Alt, A.; Weiss, B.; Ogden, A. M.; Knauss, J. L.; Oler, J.; Ho, K.; Large, T. H.; Bleakman, D. *Neuropharmacol.* **2004**, 46 (6), 793.
(34) Weinrich, T.; Gränz, M.; Grünewald, C.; Prisner, T. F.; Göbel, M. W. *Eur. J. Org. Chem.* **2017**, 2017 (3), 491.
(35) Tian, Z.; Menard, F. *J. Org. Chem.* **2018**, 83 (11), 6162.
(36) Nicolaou, K. C.; Estrada, A. A.; Zak, M.; Lee, S. H.; Safina, B. S. *Angew. Chem. Int. Ed.* **2005**, 44 (9), 1378.
(37) Ganguly Ghosh, B. B.; Talukdar, G.; Sharma, A. *Mutat. Res. Lett.* **1992**, 282 (2), 61.
(38) Wang, X.; Gao, Y.; Xu, Y.; Li, L.; Zhang, Z.; Liu, J. *Syn. Comm.* **2009**, 39 (22), 4030.
(39) Ellis-Davies, G. C. R. *Nat. Methods* **2007**, 4 (8), 619.
(40) Schmidt, R.; Geissler, D.; Hagen, V.; Bendig, J. *J. Phys. Chem. A* **2007**, 111 (26), 5768.
(41) Schmidt, R.; Geissler, D.; Hagen, V.; Bendig, J. *J. Phys. Chem. A* **2007**, 111 (26), 5768.
(42) Guruge, C.; Ouedraogo, Y. P.; Comitz, R. L.; Ma, J.; Losonczy, A.; Nesnas, N. *ACS Chem. Neurosci.* **2018**, 9 (11), 2713.
(43) Verkhratsky, A.; Kirchhoff, F. *J. Anat.* **2007**, 210 (6), 651.
(44) Chung, W.-S.; Allen, N. J.; Eroglu, C. *Cold Spring Harb. Perspect. Biol.* **2015**, 7 (9), a020370.
(45) Allen, N. J.; Neuron, C. E.; *Neuron.* **2017**, 96(3), 697.
(46) Bernardinelli, Y.; Randall, J.; Janett, E.; Nikonenko, I.; König, S.; Jones, E. V.; Flores, C. E.; Murai, K. K.; Bochet, C. G.; Holtmaat, A.; Muller, D. *Curr. Biol.* **2014**, 24 (15), 1679.
(47) Haber, M.; Zhou, L.; Murai, K. K. *J. Neurosci.* **2006**, 26 (35), 8881.
(48) Stevens, B. *Neurosignals* **2008**, 16 (4), 278.
(49) Barker, A. J.; Ullian E.M. *Neuroscientist*, **2010**.
(50) Cornell-Bell, A. H.; Thomas, P. G.; Caffrey, J. M. *Can. J. Physiol. Pharmacol.* **1992**, 70 (S1), S206.
(51) Bell, A. H. C.; Thomas, P. G.; Smith, S. *J. Glia* **1990**, 3 (5), 322.
(52) Iino, M.; Goto, K.; Kakegawa, W.; Okado, H.; Sudo, M.; Ishiuchi, S.; Miwa, A.; Takayasu, Y.; Saito, I.; Tsuzuki, K.; Ozawa, S. *Science* **2001**, 292 (5518), 926.

Optical Control of Ca^{2+}-Mediated Morphological Response in Glial Cells with Visible Light Using a Caged Kainoid

Zhenlin Tian,[#,†] Mitra Tabatabaee,[#,‡] Simon Edelmann,[†] Julien Gibon [§] and Frederic Menard[*,†,‡]

[†] Department of Chemistry, [‡] Department of Biochemistry & Molecular Biology, [§] Department of Biology, I.K. Barber School of Sciences, The University of British Columbia, Kelowna, BC, Canada V1V 1V7

Supporting information

Table of Contents

1. General Information

General Experimental Procedures. Unless otherwise noted, reactions were carried out under an argon atmosphere, in flame-dried single-neck, round bottom flasks fitted with a rubber septum and with magnetic stirring. Air or water sensitive liquids and solutions were transferred via syringe or stainless steel cannula. Organic solutions were concentrated by rotary evaporation at 25–45 °C at 50–200 torr. Thin layer chromatography (TLC) was performed on glass plates precoated with Silica gel F254, 250 μm, 60 Å, from EMD Chemicals Inc (EMD 5715-1). TLC plates were visualized under a 254 or 365 nm UV light source, then stained by immersion in either acidic aqueous-ethanolic vanillin solution, potassium permanganate, or acidic ethanolic ninhydrin, followed by heating using a heat gun. Purification was performed with 230-400 mesh silica gel from Silicycle, Quebec (SiliaFlash R12030B, P60, 40-63 μm, 60 Å).

Materials. Reagents and starting materials were purchased from: Sigma-Aldrich, Oakwood Chemicals, Alfa Aesar, Acros Organics, TCI America, or Fisher Scientific and were used as received unless otherwise noted. Tetrahydrofuran, dichloromethane, hexanes, toluene, and diethyl ether were purified on a glass contour solvent purification system under an argon atmosphere. Methanol was dried by allowing it to stand over freshly activated 4 Å molecular sieves for 48 hours prior to use. Solvents used for chromatographic purifications were obtained from Fischer Scientific or VWR and used without further purification. All new compounds (12–17) and final products (2– 4) were characterized with 1D (^{1}H NMR and ^{13}C NMR) and 2D NMR (COSY, HSQC, HMBC) spectroscopic analyses.

Instruments. ^{1}H and ^{13}C NMR spectra were recorded on a 400 MHz Varian NMR AS400 equipped with an ATB-400 probe at 25 °C. NMR spectra were analyzed with MestReNova Version 10.0 from Mestrelab Research. Chemical shifts are reported in parts per million (ppm, δ scale) downfield from tetramethylsilane and are referenced to residual proton signals in the NMR solvents ($CHCl_3$: δ 7.26, C_2HD_5SO: δ 2.50), for carbons ($CDCl_3$: δ 77.0, C_2HD_5SO: δ 39.5). Spectral data are listed as follows: chemical shift, integration, multiplicity (s = singlet, d = doublet, t = triplet, q = quartet, m = multiplet, br s= broad singlet), and coupling constant (*J*, Hz). Infrared spectra (IR) were obtained using a Perkin-Elmer FT-IR Spectrum Two IR spectrometer as a neat film on a NaCl plate. High resolution mass spectra were obtained from the McMaster Regional Center for Mass Spectrometry using a Waters Micromass LCT Premier TOF Mass Spectrometer.

2. Synthesis Procedures & Characterization Data

2.1 Synthesis of coumarinyl cage reagents

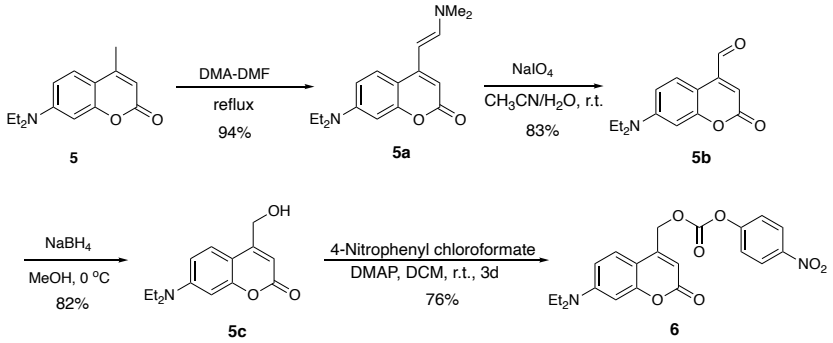

Scheme S1. Synthesis of coumarinyl reagents

(*E*)-7-(Diethylamino)-4-(2-(dimethylamino)vinyl)-2*H*-chromen-2-one (5a). To a solution of coumarin **5** (10.00 g, 43.23 mmol) in dry DMF (50 mL) was added *N,N*-dimethylformamide dimethyl acetal (4.60 mL, 34.6 mmol). The reaction mixture was then refluxed overnight. The reaction mixture was poured into water. It resulted a large amount of brown precipitation, the solid product was collected by vaccum filtration. The solid was further washed with ether (30 mL) to afford enamine **5a** as a dark-yellow solid (11.64, 94%). The crude product was used as is directly for the next step. Characterization data matched literature precedents.[1]

FTIR (neat, thin film): 2968, 2930, 2876, 2817, 1678, 1605, 1566, 834, 817, 793, 772 cm^{-1}.

^{1}H NMR (400 MHz, $CDCl_3$): δ 7.53 (d, *J* = 9.0 Hz, 1H), 7.22 (d, *J* = 13.0 Hz, 1H), 6.55 (dd, *J* = 9.0, 2.7 Hz, 1H), 6.49 (d, *J* = 2.6 Hz, 1H), 5.85 (s, 1H), 5.22 (d, *J* = 13.0 Hz, 1H), 3.40 (q, *J* = 7.1 Hz, 4H), 2.99 (s, 6H), 1.20 (t, *J* = 7.1 Hz, 6H) ppm.

^{13}C NMR (101 MHz, $CDCl_3$): δ 163.6, 156.4, 152.4, 150.1, 146.6, 124.8, 108.1, 107.9, 98.1, 93.4, 87.5, 44.7, 12.5 ppm.

7-(Diethylamino)-2-oxo-2*H*-chromene-4-carbaldehyde (**5b**). Enamine **5a** (2.0 g, 6.9 mmol) was dissolved in acetonitrile (5 mL). To this solution was added H_2O (5 mL) and $NaIO_4$ (1.6 g, 7.7 mmol). The mixture was stirred at rt for 30 mins, TLC showed the full conversion. The reaction mixture was poured into water and extracted with ethyl acetate (3 × 50 mL). The combined organic layer was washed with brine, dried over $MgSO_4$ and filtered. The solvent was removed under reduced pressure. The residue was purified by column chromatography using ethyl acetate / hexane as eluent (20-60% gradient). Aldehyde **5b** was recovered as an orange solid (1.4 g, 83%). Characterization data matched literature precedents.[1]

^{1}H NMR (400 MHz, $CDCl_3$): δ 10.03 (s, 1H), 8.31 (d, *J* = 9.2 Hz, 1H), 6.63 (dd, *J* = 9.2, 2.6 Hz, 1H), 6.53 (d, *J* = 2.7 Hz, 1H), 6.45 (s, 1H), 3.43 (q, *J* = 7.1 Hz, 4H), 1.22 (t, *J* = 7.1 Hz, 6H) ppm.

[1] *Eur. J. Org. Chem.*, **2017** (3), 491-496.

^{13}C NMR (101 MHz, $CDCl_3$): δ 192.5, 161.9, 157.4, 151.0, 143.9, 127.0, 117.4, 109.5, 103.7, 97.6, 44.8, 12.5 ppm.

7-(Diethylamino)-4-(hydroxymethyl)-2*H*-chromen-2-one (5c). To a solution of aldehyde **5b** (1.201 g, 4.89 mmol) in methanol (5 mL) was added sodium borohydride (93 mg, 2.5 mmol) at 0 ^{O}C. After 30 mins, TLC showed the full conversion. The mixture was quenched with ammonium chloride aqueous solution and extracted with ether (3 × 30 mL). The combined organic layer was washed with sodium bicarbonate aqueous solution and brine. The ether layer was dried over $MgSO_4$ and filtered. The filtrated was concentrated to dryness under reduced pressure and afford the alcohol **5c** as a yellow solid (993 mg, 82%) without further purification. Characterization data matched literature precedents.[2]

FTIR (neat, thin film): 3446, 2971, 1739, 1686, 831, 798 cm^{-1}.

^{1}H NMR (400 MHz, $CDCl_3$): δ 7.30 (d, *J* = 9.0 Hz, 1H), 6.55 (d, *J* = 9.0 Hz, 1H), 6.45 (s, 1H), 6.28 (s, 1H), 4.82 (s, 2H), 3.38 (q, *J* = 6.9 Hz, 4H), 1.18 (t, *J* = 7.3 Hz, 6H) ppm.

^{13}C NMR (101 MHz, $CDCl_3$): δ 163.1, 156.1, 155.5, 150.5, 124.4, 108.7, 106.4, 105.2, 97.6, 60.8, 44.7, 12.5 ppm.

HRMS (ESI) m/z: $[M + Na]^+$ calcd for $C_9H_{10}NO_4Na$, 270.1101; found, 270.1094.

(7-(Diethylamino)-2*H*-chromen-4-yl)methyl (4-nitrophenyl) carbonate (6). To a single-neck flask were added 4-nitrophenyl chloroformate (1.61 g, 7.99 mmol), alcohol **5c** (659 mg, 2.66 mmol), DMAP (326 mg, 2.66 mmol) and dichloromethane (5 mL) at rt. The flask was then purged with argon and covered with foil to avoid light. After 2 d, the reaction mixture was poured into water and extracted with ethyl acetate (50 mL × 3). The combined organic layer was then washed with brine and dried over $MgSO_4$. The organic solvent was removed under reduced pressure. The resulted residue was then washed diethyl ether (50 mL) to remove unreacted alcohol and afforded the carbonate **6** (833 mg, 76%) as a yellow solid without further purification. The product was stored in a foil covered vail.

FTIR (neat, thin film): 2972, 1774, 1711, 862, 839, 752 cm^{-1}.

^{1}H NMR (400 MHz, $CDCl_3$): δ 8.31 (d, *J* = 9.1 Hz, 2H), 7.42 (d, *J* = 9.1 Hz, 2H), 7.32 (d, *J* = 9.0 Hz, 1H), 6.61 (dd, *J* = 9.0, 2.6 Hz, 1H), 6.54 (d, *J* = 2.6 Hz, 1H), 6.23 (s, 1H), 5.40 (d, *J* = 1.2 Hz, 2H), 3.43 (q, *J* = 7.1 Hz, 4H), 1.22 (t, *J* = 7.1 Hz, 6H) ppm.

^{13}C NMR (101 MHz, $CDCl_3$): δ 161.6, 156.4, 152.2, 150.9, 147.6, 125.4, 124.3, 121.7, 108.8, 107.0, 105.6, 98.0, 65.8, 44.8, 12.4 ppm.

[2] *Eur. J. Org. Chem.*, **2017** (3), 491-496.

2.2 Synthesis of MNI-Glu

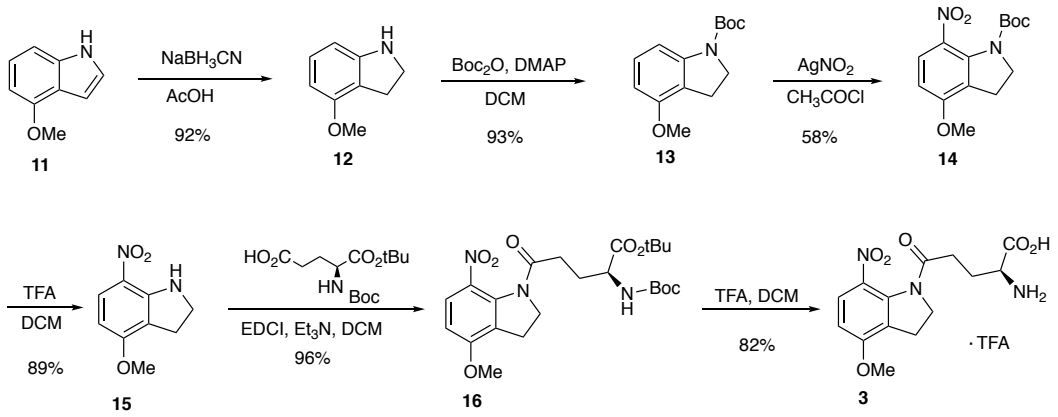

Scheme S2. Synthesis of MNI-Glu

(*S*)-2-Amino-5-(4-methoxy-7-nitroindolin-1-yl)-5-oxopentanoic acid, MNI-Glu (**3**) was prepared according to a modified literature procedure. Characterization data matched literature precedents.[3,4]

^{1}H NMR (400 MHz, D_2O): δ = 7.67 (d, *J* = 9.1 Hz, 1H), 6.78 (d, *J* = 9.2 Hz, 1H), 4.17 (t, *J* = 7.9 Hz, 2H), 3.81 (s, 3H), 3.65 (t, *J* = 6.3 Hz, 1H), 2.96 (t, *J* = 7.9 Hz, 2H), 2.64 (t, *J* = 7.5 Hz, 2H), 2.04 (q, *J* = 7.1 Hz, 2H) ppm.

2.3 Synthesis of DECM-Glu

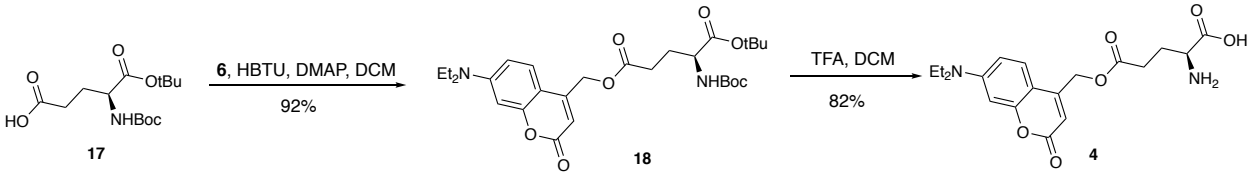

Scheme S3. Synthesis of DECM-Glu

1-(*tert*-Butyl) 5-((7-(diethylamino)-2-oxo-2*H*-chromen-4-yl)methyl)(*tert*-butoxycarbonyl)-*L*-glutamate (18) was prepared according to a modified literature procedure.[5] Characterization data matched literature precedents. To a solution of Boc-Glu-OtBu (245 mg, 0.808 mmol) in dichloromethane (5 mL) were added alcohol **6** (241 mg, 0.972 mmol), HBTU (306 mg, 0.807 mmol) and triethylamine (115 μL, 0.808 mmol). The reaction was stirred under argon atmosphere at rt (the flask was cover with foil to avoid light irradiation) for 3 d. Then the reaction mixture was poured into water and extracted with ethyl acetate (3 × 20 mL). The combined organic layer was washed with ammonium chloride aqueous solution, sodium bicarbonate aqueous solution and brine. The resulting organic layer was dried over $MgSO_4$ and filtered. The filtrate was concentrated under

[3] *Syn. Comm.* **2009**, 39(22), 4030-4038.
[4] *Chem. Comm.* **2005**, 0 (29), 3664-3666.
[5] *Biochemistry*. **2005**, 44(19), 7107-7114.

reduced pressure (a foil was used to cover the flask when removing solvent on the rotavap). The resulting residue was purified by column chromatography using ethyl acetate / hexane as an eluent (10-60% gradient). Ester **18** was recovered as a yellow solid (395 mg, 92%). Characterization data matched literature precedents.[6]

^{1}H NMR (400 MHz, $CDCl_3$): δ 7.29 (d, *J* = 9.4 Hz, 1H), 6.58 (dd, *J* = 9.0, 2.5 Hz, 1H), 6.52 (d, *J* = 2.6 Hz, 1H), 6.12 (s, 1H), 5.23 (s, 2H), 5.10 (d, *J* = 8.3 Hz, 1H), 4.28 – 4.23 (m, 1H), 3.42 (q, *J* = 7.1 Hz, 4H), 2.64 – 2.44 (m, 2H), 2.27-2.16 (m, 1H), 1.99 -1.90 (m, 1H), 1.44 – 1.49 (m, 18H), 1.21 (t, *J* = 7.1 Hz, 6H) ppm.

^{13}C NMR (101 MHz, $CDCl_3$): δ 172.1, 161.8, 156.3, 150.7, 149.2, 124.4, 108.7, 106.6, 106.0, 97.8, 82.4, 79.9, 61.6, 53.2, 44.7, 30.1, 28.3, 28.1, 28.0, 12.4 ppm.

(*S*)-2-Amino-5-((7-(diethylamino)-2-oxo-2*H*-chromen-4-yl)methoxy)-5-oxopentanoic acid (4). Ester **18** (395 mg, 0.742 mmol) was dissolved in dichloromethane (2.0 mL). Trifluoroacetic acid (1.7 mL, 22 mmol) was added dropwise. The resulting mixture was stirred at rt under argon. The flask was covered with foil and maintained for 4 h. The solvent was removed under reduced pressure (foil was used to cover the flask when removing solvent on the rotavap). The resulting residue was triturated in ether and yielded a yellow precipitation. It was filtered and solid precipitate was collected as the TFA salt of **4** (298 mg, 82%) without further purification. Characterization data matched literature precedents.[6]

FTIR (neat, thin film): 3461, 3016, 2971, 1738 cm^{-1}.

^{1}H NMR (400 MHz, CD_3OD): δ 7.47 (d, *J* = 9.1 Hz, 1H), 6.74 (dd, *J* = 9.1, 2.6 Hz, 1H), 6.55 (d, *J* = 2.7 Hz, 1H), 6.06 (s, 1H), 5.40 – 5.28 (m, 2H), 3.80 (t, *J* = 6.5 Hz, 1H), 3.48 (q, *J* = 7.1 Hz, H), 2.84 – 2.67 (m, 2H), 2.21 (dtd, *J* = 18.3, 14.2, 12.8, 7.3 Hz, 2H), 1.21 (t, *J* = 7.1 Hz, 6H) ppm.

^{13}C NMR (101 MHz, CD_3OD): δ 156.1, 151.2, 151.1, 124.8, 109.0, 105.7, 104.7, 96.9, 61.4, 44.2, 29.2, 26.7, 25.6, 11.3 ppm.

^{19}F NMR (376 MHz, D_2O) δ -75.65.

[6] *Biochemistry*. **2005**, 44(19), 7107-7114.

2.4 Synthesis of DECM-PhKA

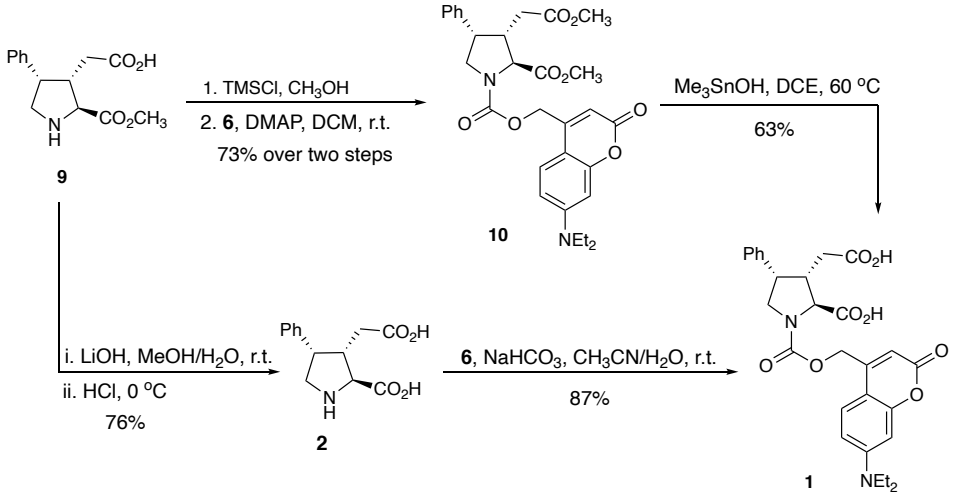

Scheme S4. Synthesis of DECM-PhKA

1-((7-(Diethylamino)-2-oxo-2*H*-chromen-4-yl)methyl) 2-methyl (2*S*,3*S*,4*S*)-3-(2-methoxy-2-oxoethyl)-4-phenylpyrrolidine-1,2-dicarboxylate (**10**). PhKA **9** was obtained from the sequence we repeated previously.[7] To the solution of **9** (25 mg, 95 μmol) in methanol (0.3 mL) was added TMSCl (30 μL, 0.24 mmol). The mixture was stirred at room temperature for 5 h. Then the solvent was removed under reduced pressure. To the resulted residue were added DMAP (17 mg, 0.14 mmol) and carbonate (38 mg, 0.095 mmol). The mixture was stirred at rt under argon atmosphere for 24 h (a foil was used to cover the whole flask during the reaction). The resulted mixture was concentrated to dryness. The resulted residue was purified by column chromatography using ethyl acetate / hexane as an eluent (20-60% gradient). The carbamate **10** was recovered as a brown solid (47 mg, 92%).

^{1}H NMR (400 MHz, $CDCl_3$, two rotamers): δ 7.37 – 7.28 (m, 4H), 7.08 (d, *J* = 7.4 Hz, 2H), 6.59 (q, *J* = 8.5, 8.1 Hz, 1H), 6.51 (s, 1H), 6.12 (d, *J* = 37.2 Hz, 1H), 5.44 – 5.15 (m, 2H), 4.25 (t, *J* = 5.9 Hz, 1H), 4.07 (q, *J* = 9.1 Hz, 1H), 3.98 – 3.87 (m, 1H), 3.82 (s, 1H), 3.77 (s, 2H), 3.63 (d, *J* = 3.9 Hz, 3H), 3.41 (d, *J* = 7.6 Hz, 1H), 3.14 – 3.06 (m, 1H), 2.35 – 2.25 (m, 1H), 2.14 – 2.04 (m, 1H), 1.21 (t, *J* = 6.7 Hz, 6H) ppm.

^{13}C NMR (101 MHz, $CDCl_3$, two rotamers): δ 172.1, 171.9, 171.9, 171.8, 162.1, 162.0, 161.8, 156.3, 156.2, 154.3, 153.9, 153.3, 150.8, 150.7, 150.7, 150.0, 149.9, 148.3, 129.0, 127.6, 127.5, 127.5, 126.1, 124.5, 124.3, 124.3, 115.7, 108.8, 108.7, 108.7, 106.9, 106.0, 105.9, 105.9, 105.8, 105.7, 97.8, 97.8, 65.3, 63.7, 63.2, 62.7, 52.7, 52.7, 51.9, 51.8, 50.7, 50.5, 45.1, 44.8, 44.7, 44.6, 44.2, 43.5, 33.2, 33.1, 12.4 ppm.

HRMS (ESI-TOF) m/z: $[M + Na]^+$ calcd for $C_{30}H_{34}N_2O_8Na$, 573.2207; found, 573.2204.

(2*S*,3*S*,4*S*)-3-(Carboxymethyl)-1-(((7-(diethylamino)-2-oxo-2*H*-chromen-4-yl)methoxy)carbonyl)-4-phenylpyrrolidine-2-carboxylic acid (1).

[7] *J. Org. Chem.* **2018**, 83(11), 6162-6170.

Method A (from **10**): To a solution of diester **10** (30 mg, 55 μmol) in dichloroethane (2 mL) was added trimethyl hydroxide (49 mg, 0.27 mmol). The mixture was refluxed overnight (the flask and condenser were covered with foils). The reaction mixture was poured into a hydrochloric acid solution (0.1 M, 10 mL) and extracted with ethyl acetate (3 × 10 mL). The combined organic layer was washed with brine, dried over $MgSO_4$ and filtered. The filtrate was concentrated and purified by column chromatography using methanol / dichloromethane as an eluent (5-20% gradient). DECM-PhKA **1** was recovered as a yellow solid (18 mg, 88%) with trace tin residues. This reaction was abandoned due to the toxicity of tin for living cells.

Method B (from **2**): The free phenylkainic acid **2** was obtained according to our prior report.[8] To a solution of PhKA **2** (76 mg, 0.30 mmol) in H_2O (1.0 mL) and acetonitrile (2.0 mL) were added sodium bicarbonate (77 mg, 0.91 mmol) and carbonate **6** (125 mg, 0.30 mmol). The mixture was stirred at rt for 24 h (the whole flask was covered with foils). The resulted solution was then poured into a hydrochloric acid solution (0.1 M, 10 mL) and extracted with ethyl acetate (3 × 20 mL). The combined organic layer was washed with brine, dried over $MgSO_4$ and filtered. The filtrate was concentrated under reduced pressure (a foil was used to cover the flask when on the rotavap). The resulted residue was triturated in ether (30 mL) and filtered to afford DECM-PhKA **1** as a yellow solid.

FTIR (neat, thin film): 3414, 2977, 1709, 1601 cm^{-1}.

^{1}**H NMR** (400 MHz, CD_3OD, two rotamers): δ 7.49 (t, *J* = 9.3 Hz, 1H), 7.32 (dt, *J* = 7.9, 4.1 Hz, 2H), 7.26 (t, *J* = 7.2 Hz, 1H), 7.13 (d, *J* = 7.2 Hz, 2H), 6.74 (ddd, *J* = 14.2, 9.1, 2.6 Hz, 1H), 6.55 (d, *J* = 2.5 Hz, 1H), 6.14 (d, *J* = 15.8 Hz, 1H), 5.47 – 5.28 (m, 2H), 4.31 – 4.09 (m, 1H), 4.07 – 3.84 (m, 1H), 3.77 (bs, 1H), 3.48 (qd, *J* = 7.0, 4.8 Hz, 4H), 3.07 (bs, 1H), 2.37 (bs, 1H), 2.06 – 1.90 (m, 1H), 1.21 (td, *J* = 7.1, 4.7 Hz, 6H) ppm.

^{13}**C NMR** (101 MHz, CD_3OD, two rotamers): δ 162.99, 156.14, 156.05, 154.00, 151.84, 151.07, 151.06, 138.54, 138.44, 128.50, 128.48, 127.46, 126.90, 124.81, 124.65, 109.08, 109.05, 105.71, 105.61, 104.77, 104.41, 96.83, 62.52, 45.02, 44.19, 31.32, 11.30 ppm.

HRMS (ESI-TOF) m/z: $[M - H]^-$ calcd for $C_{28}H_{29}N_2O_8$, 521.1929; found, 521.1906.

[8] *J. Org. Chem.* **2018**, 83(11), 6162-6170.

3. Photochemical Characterization of Photocaged Agonists

The photochemical properties of caged KAR agonists MNI-Glu **3**, DECM-Glu **4** and DECM-PhKA **1** were measured along with their photolysis rates. The photolysis experiments were carried out with two types of blue LED photochemical reactors (custom-made in our lab). One reactor had its maximum irradiation wavelength centered at 465 nm, and the other at 445 nm. Both lamps' irradiation range overlapped partially with the absorption ranges of DECM-Glu and DECM-PhKA, but there was almost no overlap with MNI-Glu (Figure S1).

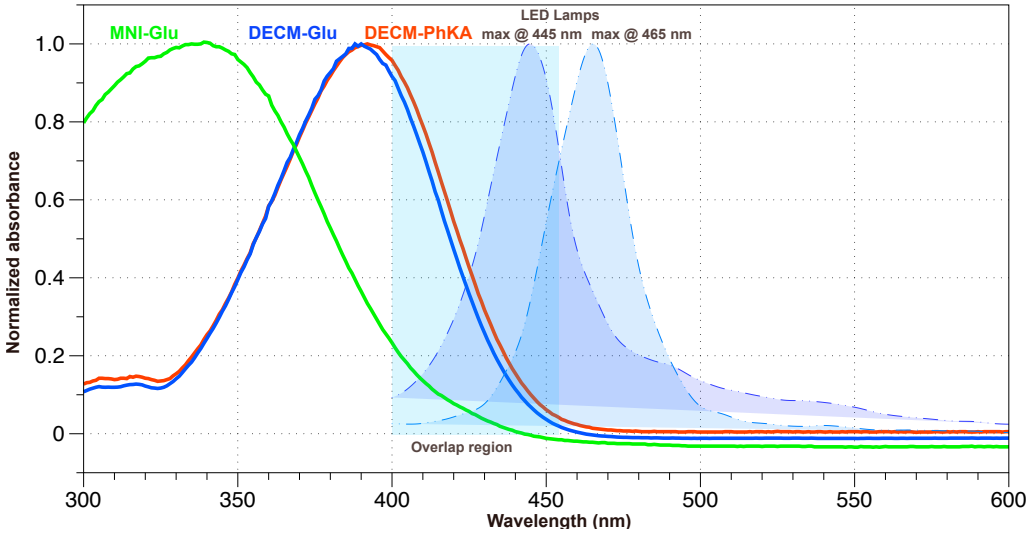

Figure S1. Overlay of the two photoreactors irradiadiation ranges (blue-shaded areas) of the absorption spectra of caged compounds **1**, **3** and **4**. The absorption of both molecules caged with a DECM coumaryl group overlap with the blue LED light sources. The smaller MNI cage group absorbs mostly in the UV range, and shows very little overlap with the light sources.

Photolysis reactions with the caged compounds **1, 3** and **4** were performed in aqueous solutions to mimic physiological conditions (0.1% DMSO/H_2O). Indeed, photochemical reactions in water are notoriously inefficient from a quantum yield standpoint, therefore it was important to measure the efficiency of our photoreactive probes in an unbiased milieu, as close as possible to their intended applications. As expected from the data shown in Figure S1, MNI-Glu showed virtually no photolysis upon irradiation with the 445 nm blue LED light source (Figure S2A). In contrast, both DECM-Glu and DECM-PhKA showed effective cleavage under same conditions after only five minutes (Figure S2B-C).

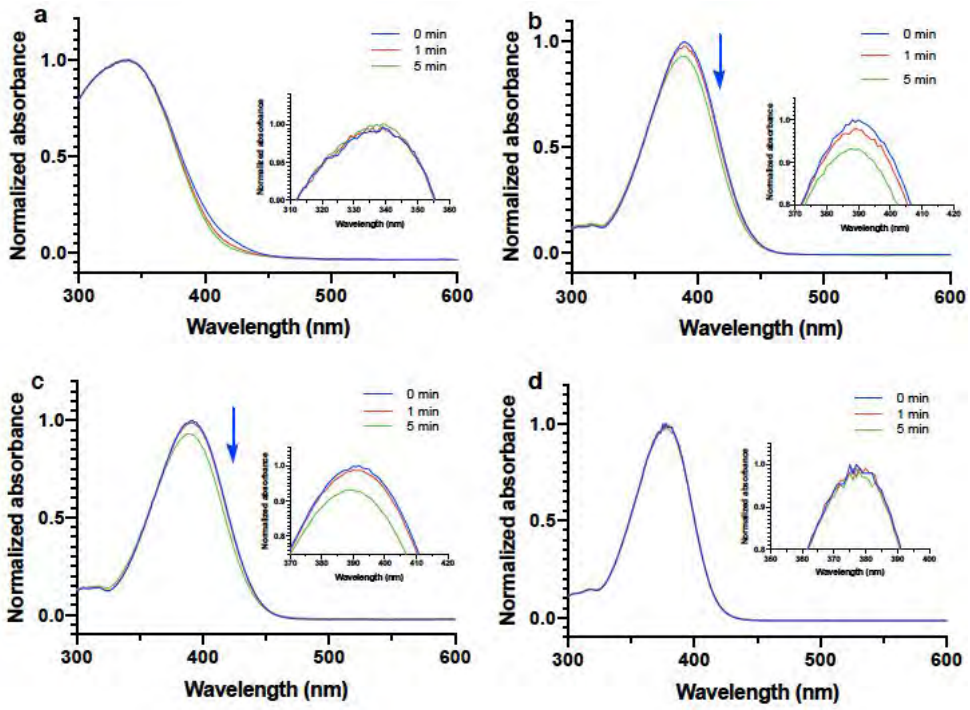

Figure S2. Time-dependent photolysis of caged compounds under blue LED light irradiation (445 nm): the absorbance of the compounds decrease as the photocage is released. (**A**) MNI-Glu in water containing 0.1% DMSO: no change in maximum absorbance is observed after 5 minutes irradiation. (**B**) DECM-Glu and (**C**) DEMC-PhKA in water containing 0.1% DMSO: both molecules display a ~10% change in absorbance after 5 minutes due to cleavage of the caged group. (**D**) DECM-PhKA in DMSO only: no photo-release takes place as water is required in the mechanism of photocehmical cleavage of the DECM coumarin.

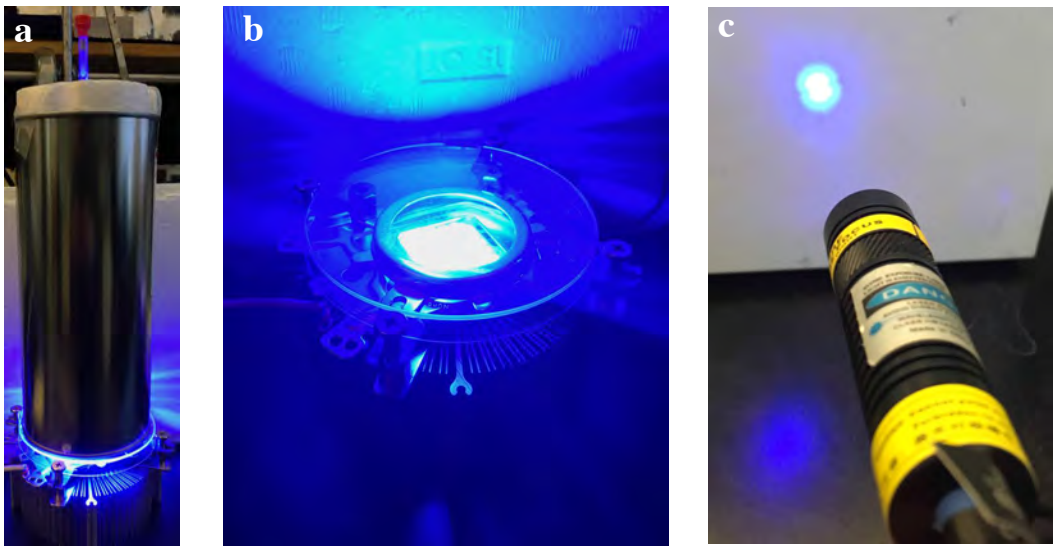

Figure S3. Photoreactors used in kinetic studies. (**A**). NMR tube in the LED photoreactor; (**B**). Blue LED reactor; (**C**). Blue laser used in kinetic studies.

As a control experiment, 445 nm irradiation of DECM-PhKA did not lead to uncaging in anhydrous DMSO . This lack of reaction is explained by the necessity for a stoichiometric amount of water in the photolysis process. A successful lysis process involves the disassociation of [CM-A] to singlet ion pair [CM^+A^-] and subsequent combination with H_2O to yield CM-OH and A^-.[6] Without H_2O, the singlet ion pair [CM^+A^-] can undergo relaxation and recombine to the ground state of CMA.

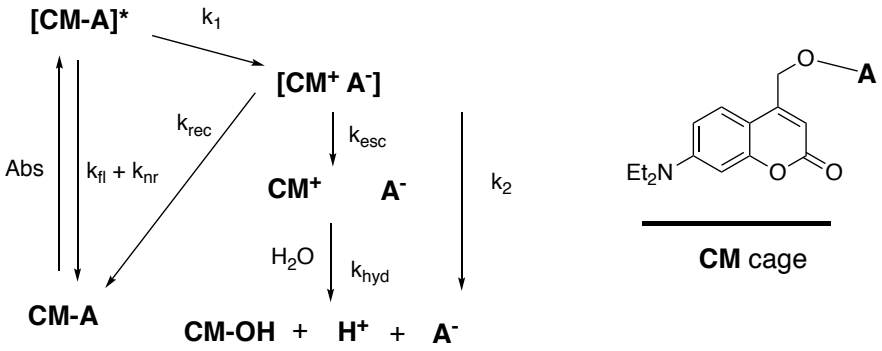

Figure S4. Proposed mechanism for the photolysis of the diethylcoumarin caged compounds under light radiation.

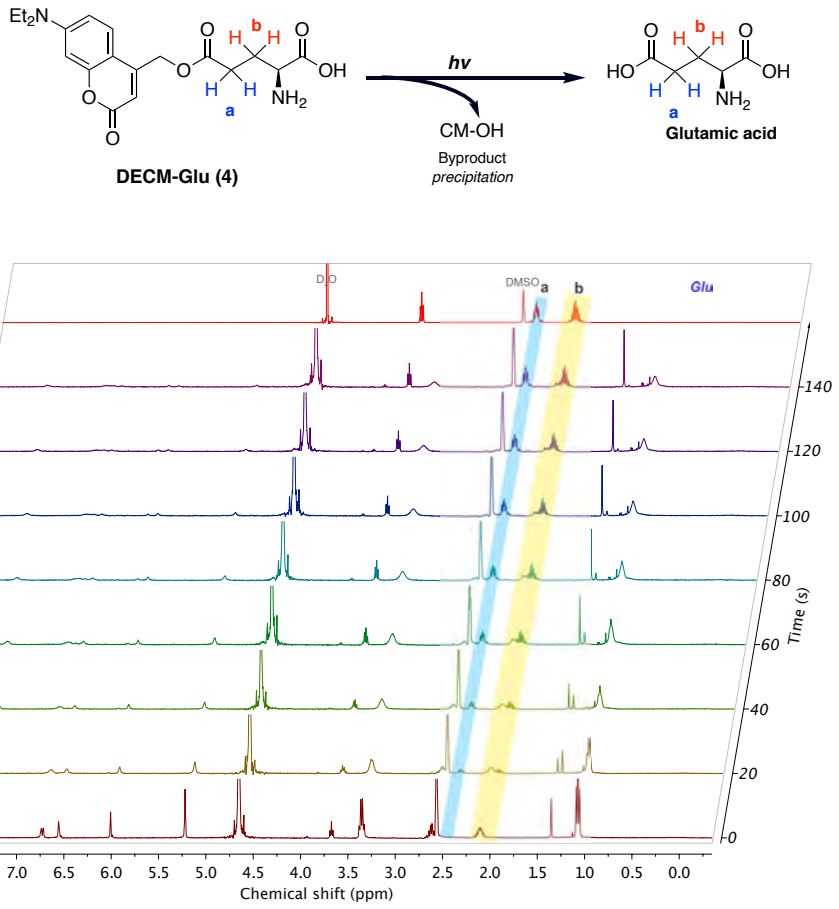

Figure S5. Overlaid ^{1}H NMR spectra of the photolysis process for DECM-Glu (**4**) as function of time irradiated with blue light (445 nm). Top spectrum is the glutamic acid reference (red traces). The depth axis shows time intervals of ^{1}H NMR spectra acquisition. CM-OH: 7-(diethylamino)-4-hydroxymethylcoumarin.

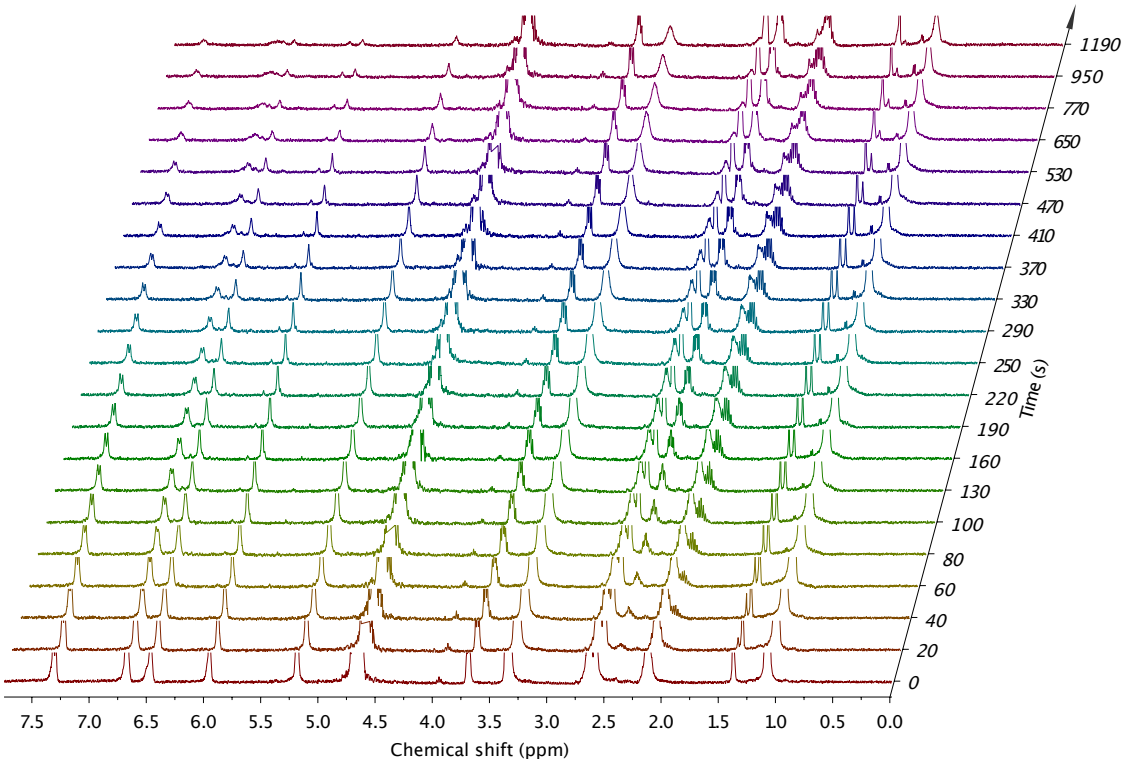

Figure S6. ^{1}H NMR spectra for progressive photolysis of DECM-Glu using a 465 nm photoreactor

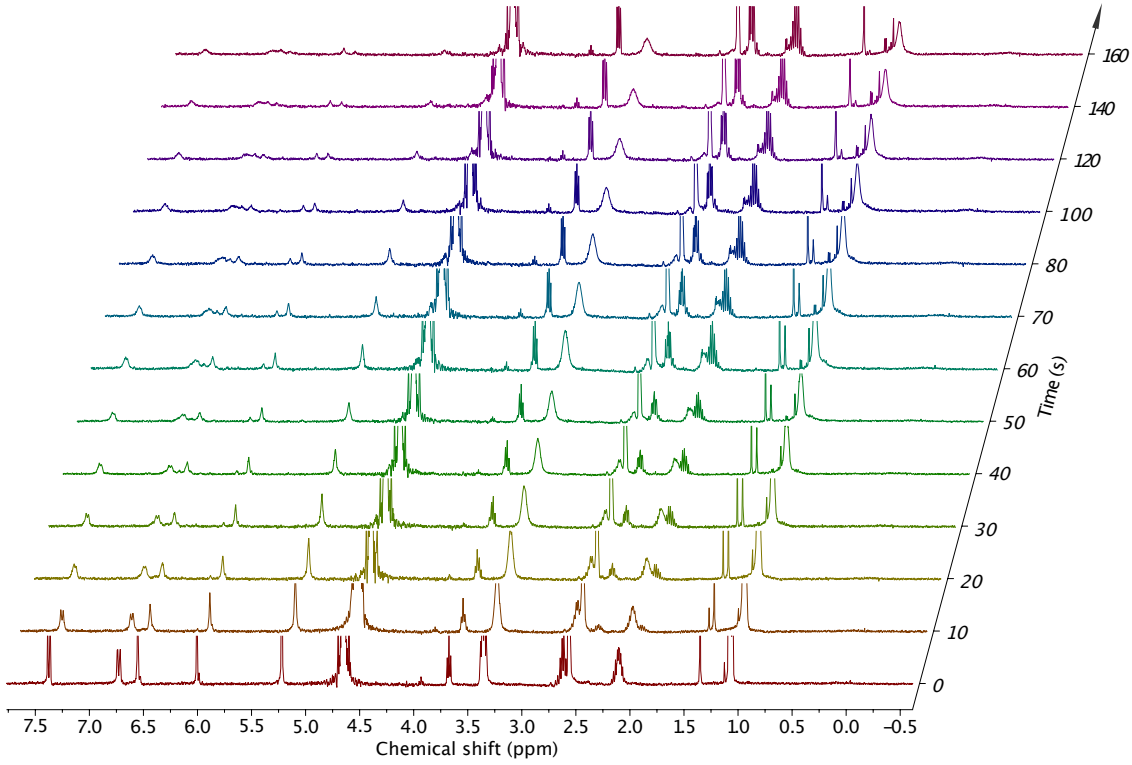

Figure S7. ^{1}H NMR spectra for progressive photolysis of DECM-Glu using 445 nm photoreactor

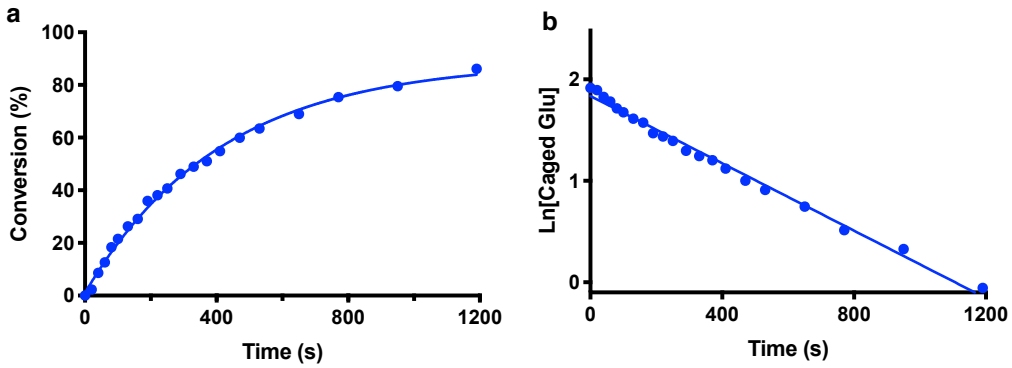

Figure S8. Photolysis rate of DECM-Glu under 465 nm photoreactor. (A) DECM-Glu photolysis conversion (using 465 nm LED lamp) versus time (calculated based on NMR data); (B) DECM-Glu photolysis (using 465 nm LED lamp) kinetic curve (calculated based on NMR data).

4. Biological Experiments

4.1 Cell culture

Human astrocytoma cell line U118-MG (HTB-15, American type Culture Collection) was generously gifted by Andis Klegeris, UBC Okanagan. Dulbecco's modified essential medium (DMEM, Lot: 2085092 Gibco Life Technology) supplemented with 10% v/v heat-inactivated fetal bovine serum (HyClone : 1628158) 1% v/v penicillin 10,000 Unit/ml streptomycin 10,000 µg/ml (Gibco Life Technology lot : 1582955) was used for cell culture. Cells were incubated in a humidified atmosphere containing 5% CO_2 at 37 ºC, and typically passaged at 80-95% confluence using a pre-warmed 0.25% trypsin-EDTA solution for 5 minutes maximum (Gibco Lot : 1572279).

For experiments, cells from a 10 cm culture dish at ~80% confluence were suspended with a pre-warmed 0.25% trypsin-EDTA solution and transferred to 35 mm glass bottom culture dishes (Mutsunami Lot#180702) in phenol red free, high glucose DMEM supplemented with 25 mM HEPES (Gibco Lot : 2027001). Enough cells were transferred to make a ~50% confluent culture-dish after their adhesion. Cells were incubated for shorter than the cells' doubling time (~33 h)[9] to block the "within variation" between samples, when different treatments were applied, for statical analysis[10] (see statistical analysis section). This period allows the cells to adopt a flattened shape after adherence that helps us define the filopodia for measurements. Identical incubation times were respected to ensure the cells were at the same growing stage in all treatments.

4.2 Transfection

U118-MG astrocytoma cells were transfected with the F-actin marker mCherry-LifeAct-7 plasmid (gift from Michael Davidson, Addgene # 54491) using a calcium phosphate precipitation protocol[11].

4.3 Treatments

On the microscope stage, U118-MG cells were stimulated with glutamate (Alfa Aesar Lot : S14 E013) : 10.00 µL of a 20X glutamate stock solution was delivered to the medium (2.0 mL) at the edge of the dish for a final concentration of 100 µM (Cornell-Bell, Prem, and Smith 1990; Aumann et al. 2017). The stock solutions of L-glutamate, KA, PhKA (made in house) were prepared in deionized millipore water and filter-sterilized through a 0.22 µm syringe filter.

[9] *Int. J. Cancer*. **1973**, 12(2), 438-451.
[10] *Nat. Methods*. **2014**, 11(7), 699-700.
[11] *Curr. Protoc. Mol. Biol*. **2003**, 63, 9.1.1-9.1.11.

The stock solutions of DECM-OH and DECM-PhKA were prepared in DMSO (vehicle) before every experiment. The solution was filter-sterilized using a 0.22 μm syringe filter. To avoid negative effect of DMSO on the cells, the stock solution was highly concentrated, thereby maintaining DMSO 0.01% v/v in the media.

4.4 Confocal microscopy and live imaging

The extension of processes was recorded on an Olympus FV1000 fluorescence confocal microscope equipped with a Plan-ApoN 60x/i.4 oil-immersion objective. Fluorescence of mCherry-lifeact-7 was observed with 581 nm excitation using a He–Ne laser (Cy3.5).

Changes in cell morphology were recorded at 60X magnification. To track the processes extension in time, every 20 second an image was acquired from the cell for a total of number of 90 frames (30 minutes).

4.5 Quantification of filopodia extension

The length of twenty filopodia per cell was measured manually using FIJI software. The filopodia that their entire arbor could be visualized throughout the imaging period were selected[12]. A filopodium's length was measured from the edge of the cell membrane to its apical end. Each measurement was done three times. The change in length was calculated by subtracting the process length of the image prior to stimulation (frame #10) from the length of the same filopodium after 20 minutes (i.e., frame #60). Glutamate was delivered to the medium 4 minutes after the beginning of imaging (at frame 12). We reported "change in the length" as the average of the change in the length of the selected filopodia per cell.

4.6 Statistical analysis

Each value represents the average changes measured from 5 cells, each from a separate culture dish (n = 5); the results are presented as the mean ± S.E.M. Significant differences among groups were determined using one-way or two-way analysis of variance (ANOVA) and *post hoc* analysis using GraphPad prism 7.04. A p value < 0.05 was considered significant. Statistically non-significant data is not starred on the plots.

When we were testing different compounds, to minimize technical variations within our samples for ANOVA analysis, we employed a "completely randomized block design"[13]. Cells of a 80-95% confluent dish were trypsinized and re-plated in several 35mm imaging dishes at once and incubated in a humidified atmosphere containing 5% CO_2 at 37 °C. The incubation time is shorter than the doubling time of the U118-MG cells (33

[12] *Cell. Mol. Neurobiol.* **2018**, 38, 371-378.
[13] *Nat. Methods.* **2014**, 11, 699-700.

hours),[14] which allows us to avoid variation of cells within passages before exposing to different treatments (Glutamate, KA, Ph Ka, DECM-OH and DECM-PhKA).

4.7 Visible light Photolysis

The 405 nm light produced by an Eleksmark power supply 12V DC, model FA02 was coupled into an optical fiber (550 μm internal diameter), which delivered the light to the cell. Using a micromanipulator, the optical fiber was precisely aimed at a cell positively transfected with the F-actin marker, mCherry-LifeAct-7 plasmid. The concentration of DECM-PhKA used was 4 mM for the results in Figure 3. PhKA was released locally in the close proximity of a single cell. The light was manually turned on time for 10 seconds. Typical light energies were 500 mV per pulse. Releasing Ph-KA elicits cellular filopodia protrusion and calcium flux in the target cell comparable with the effect of pure glutamate, KA and PhKA that were perfused in the media by micropipettes (Figure 4).

4.8 Live Ca^{2+} imaging with Fluo-4

U118 cells grown on a glass-bottom dish were incubated with 1.8 μM of Fluo-4 AM (Invitrogen, dissolve in DMSO, final concentration of DMSO less than 0.1%) for 10 min in an incubator at 37 °C, 5% CO_2. Cells were then washed twice with phenol red free DMEM (Gibco Lot: 2027001) and kept in the same incubator for 20 minutes to allow de-esterification of the dye. Cells were then washed twice using DMEM and the media was replaced by a phenol red free DMEM containing DECM or DECM-PhKA (final concentration of 2 mM). Before imaging the media was replaced with HBSS supplemented with 2 mM Ca^{2+}. Fields of view with at least 10 cells were acquired using a 20X objective. Images were recorded at a rate of one frame every 5 s using an inverted epifluorescence microscope (Zeiss, Axio ObserverZ.1, controlled by the ZEN2 software). The baseline fluorescence was recorded before the application of light (laser 400-460 nm wavelength) for at least 1:00 min and average (F0). ImageJ software (NIH ImageJ, FIJI) was used to correct for background fluorescence for each frame by averaging the pixel intensity value of three background regions and subtracting this value from the mean pixel intensity of the uncorrected frame. The changes in Fluo-4 fluorescence as a function of time were expressed as F/F0, with F being the Fluo-4 fluorescence.

[14] *Int. J. Cancer*. **1973**, 12, 438-451.

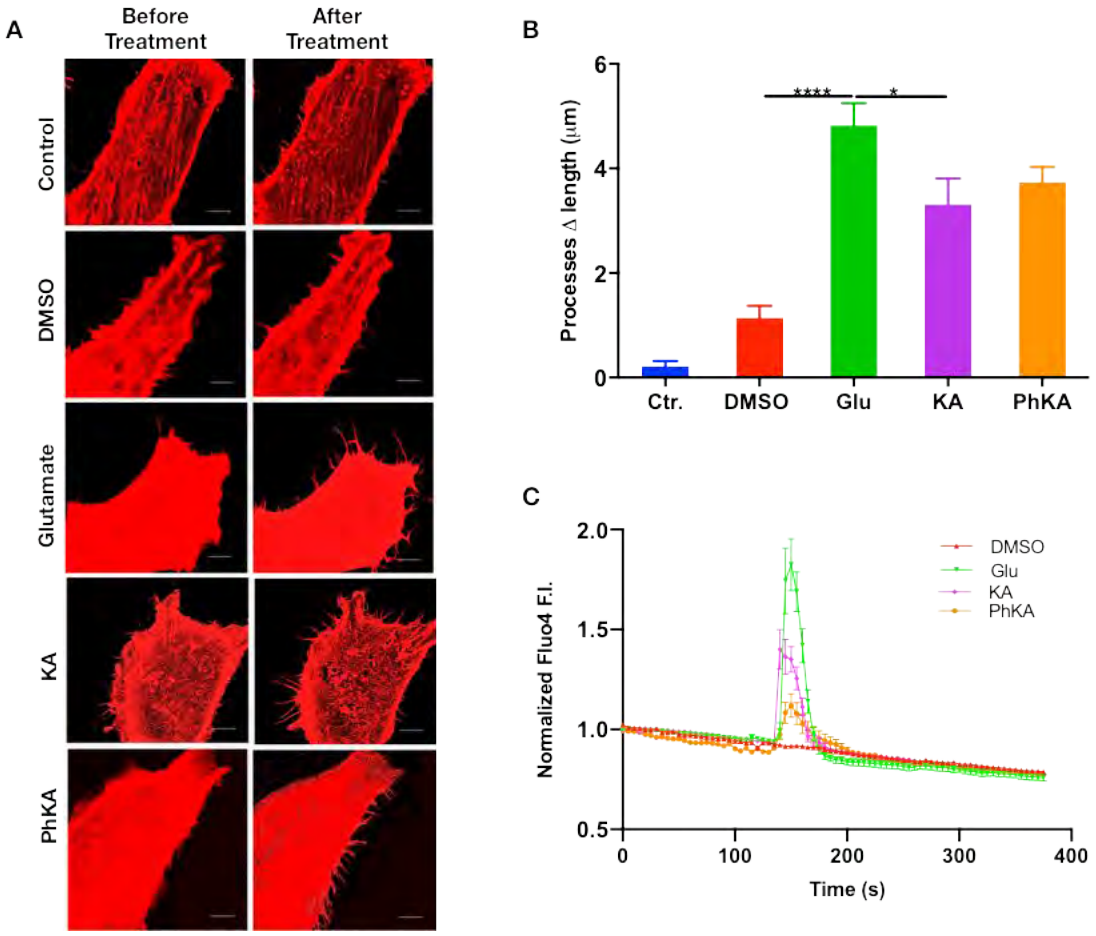

Figure S9. **Control experiments for filopodia extension and calcium flux in model astrocytes.** (**A**) Representative images of U118-MG astrocytoma cells upon exposure to 100 μM glutamate, kainic acid, PhKA, and DECM-PhKA. Confocal fluorescence micrographs of cells transfected with mCherry-LifeAct7 at 60X magnification; scale bar is 10 μM. (**B**) Cells extend their processes significantly in response to 100 μM glutamate. Change in length (Δ) was calculated by subtracting the length of a filopodium immediately prior to stimulation from that of the same filopodium after 20 minutes. The change in length is the average data of 5 cells, each from a separate culture dish; measurements of at least 20 filopodia were averaged for each cell (n = 5). Results are presented as mean ± SEM. All comparisons done by post hoc Tukey's multiple comparison (one-way ANOVA), ****p < 0.0001. (**C**) Intracellular calcium signals following applying 100μM of PhKA, KA, glutamate and DMSO (as the vehicle) on Fluo4-AM filled U118-MG cells (n=3 independent dishes, ~100 cells). Results are presented as mean ± SEM.

5. NMR Spectra

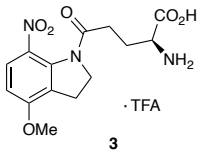

3 ^{1}H NMR (400 MHz, D_2O, 25 °C)

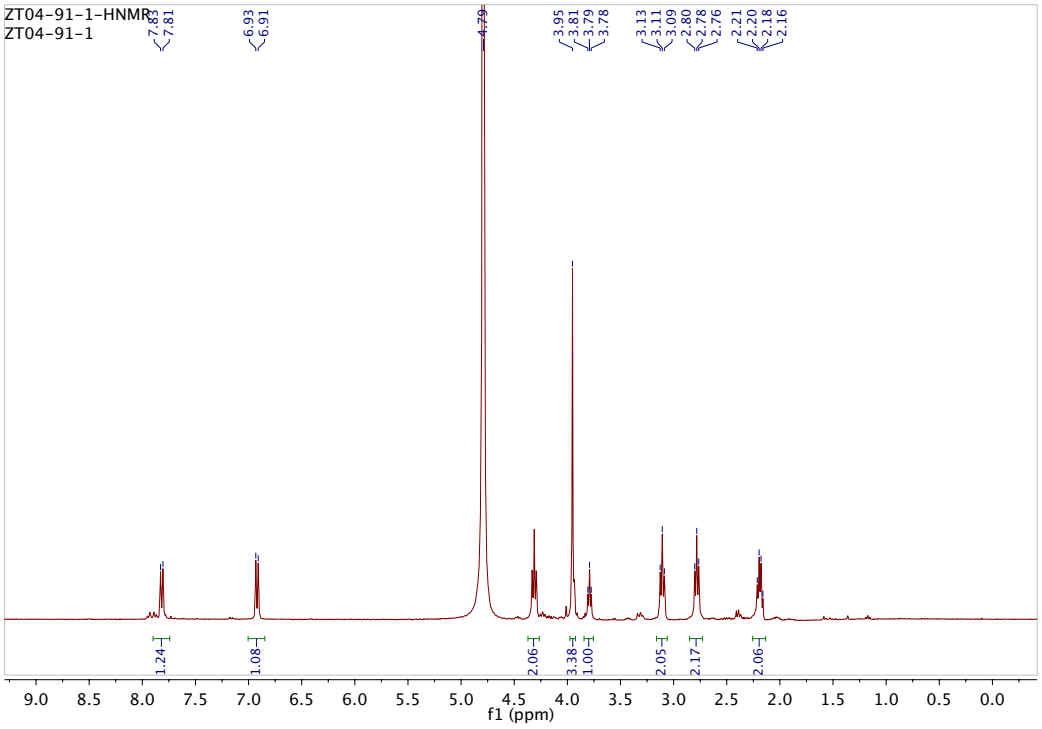

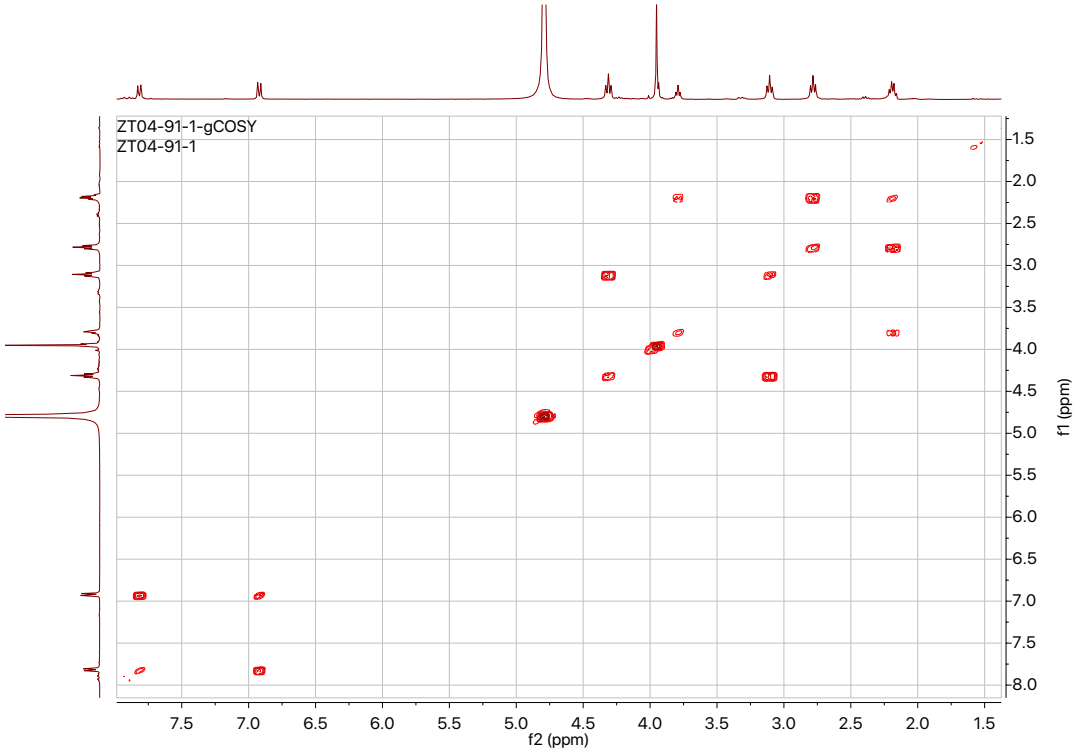
ZT04-91-1-gCOSY
ZT04-91-1
f2 (ppm)
f1 (ppm)

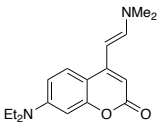

5a

^{1}H NMR (400 MHz, $CDCl_3$, 25 °C)

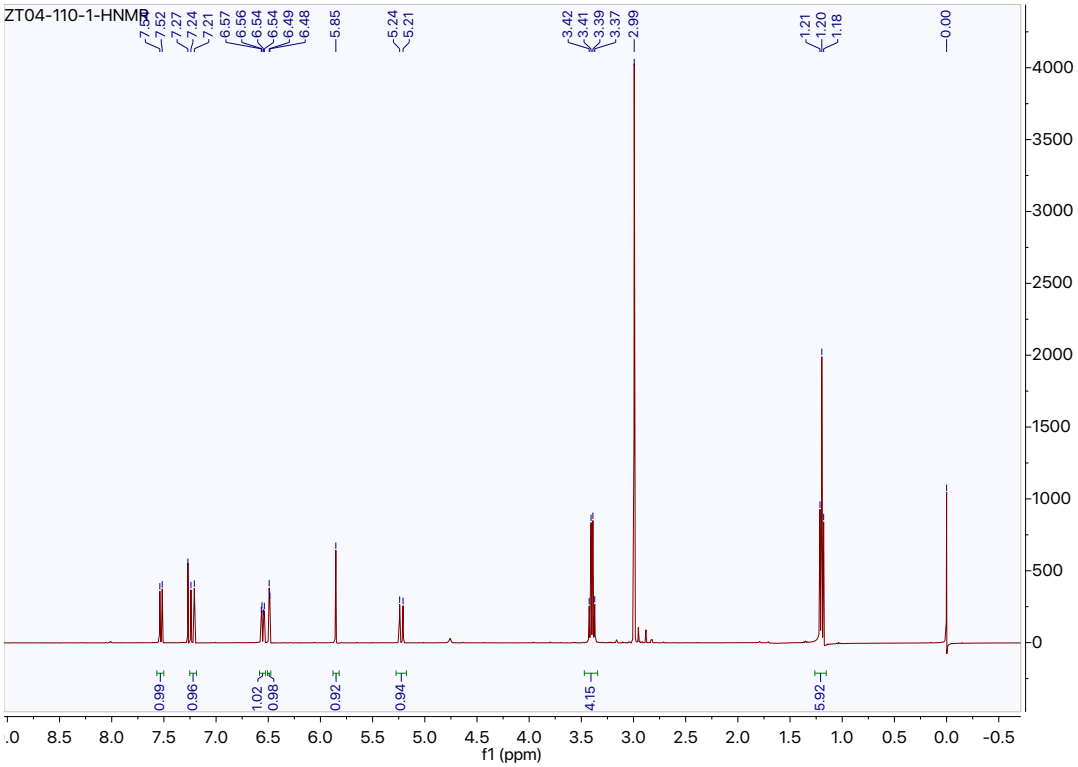

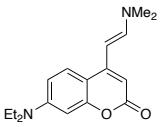

5a

^{13}C NMR (101 MHz, $CDCl_3$, 25 °C)

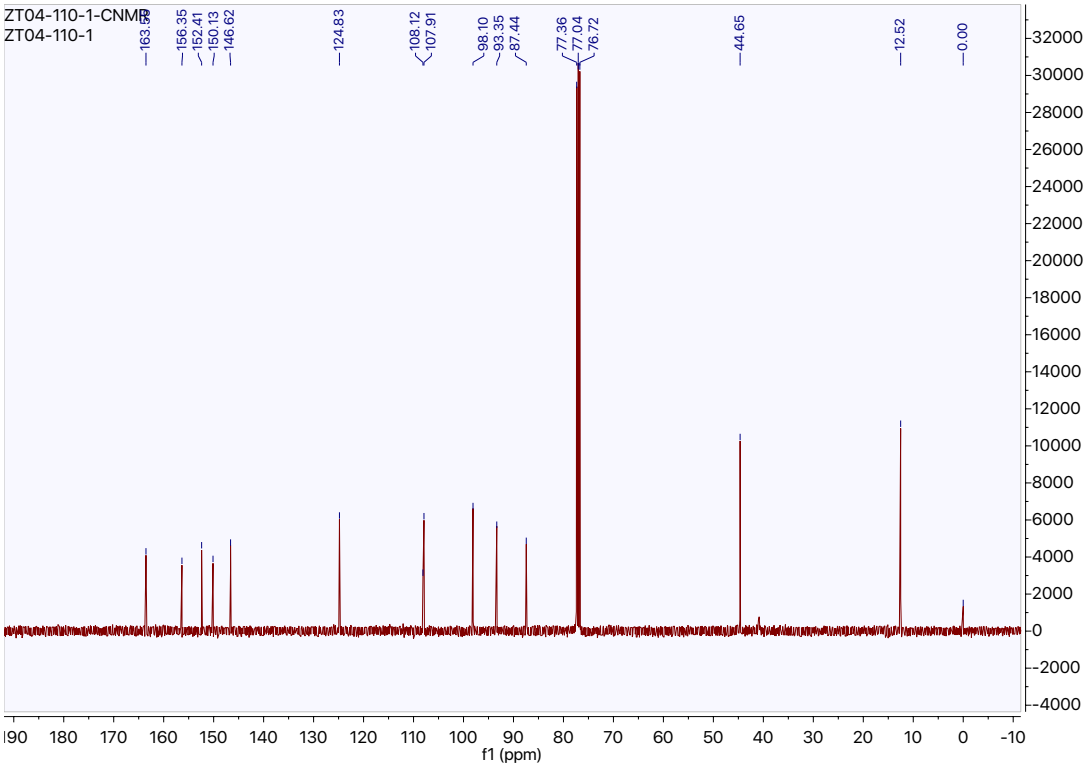

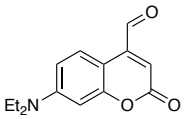

5b ^{1}H NMR (400 MHz, $CDCl_3$, 25 °C)

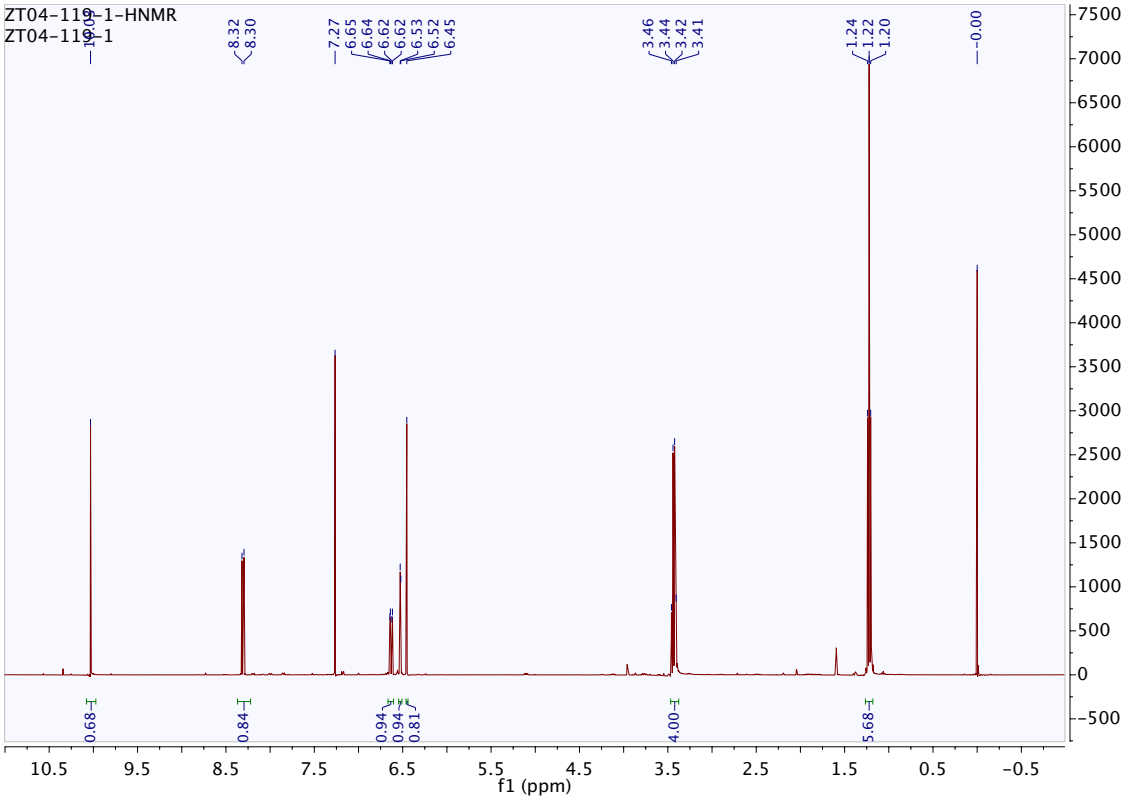

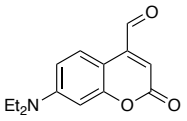

5b ^{13}C NMR (101 MHz, $CDCl_3$, 25 °C)

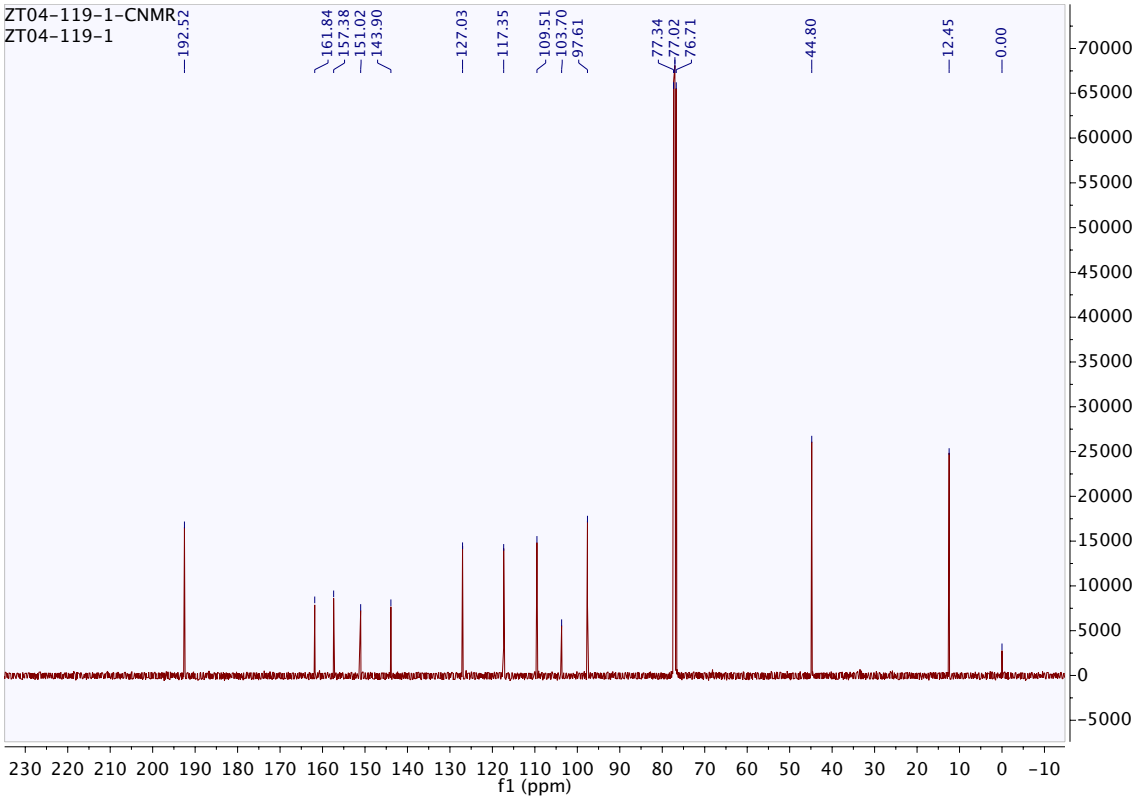

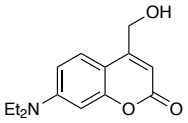

5c ^{1}H NMR (400 MHz, $CDCl_3$, 25 °C)

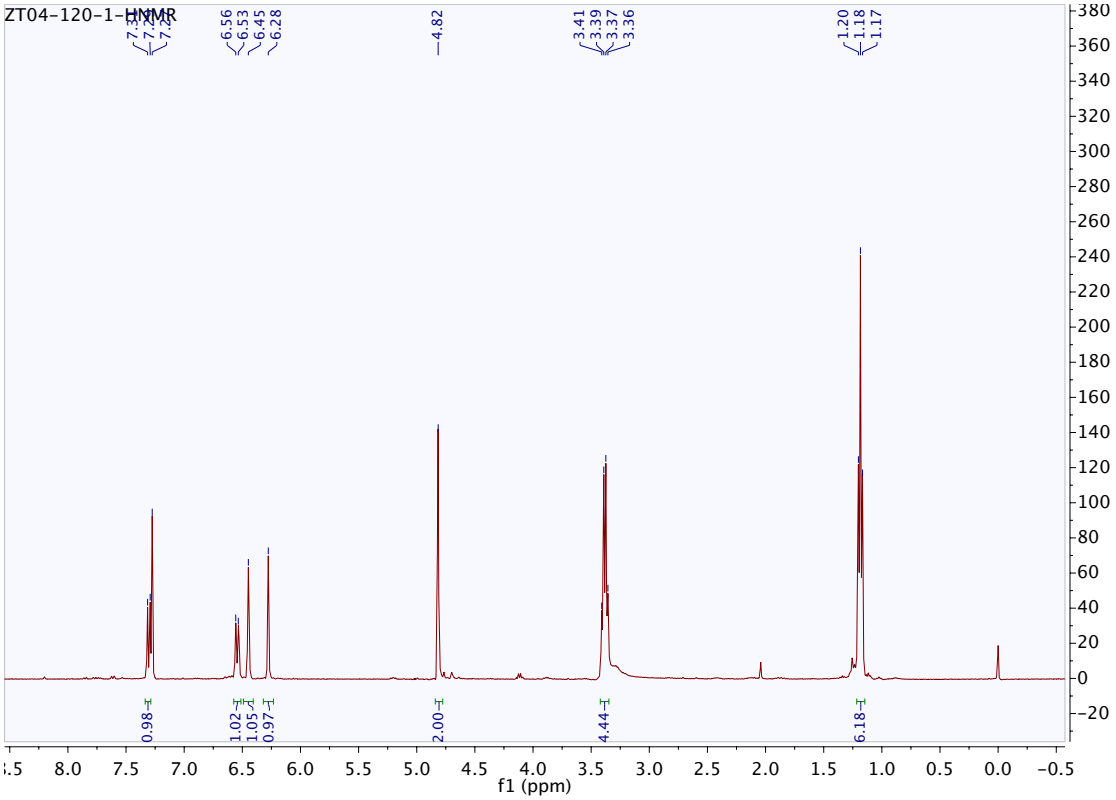

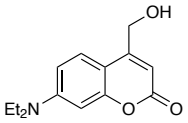

5c

^{13}C NMR (101 MHz, $CDCl_3$, 25 °C)

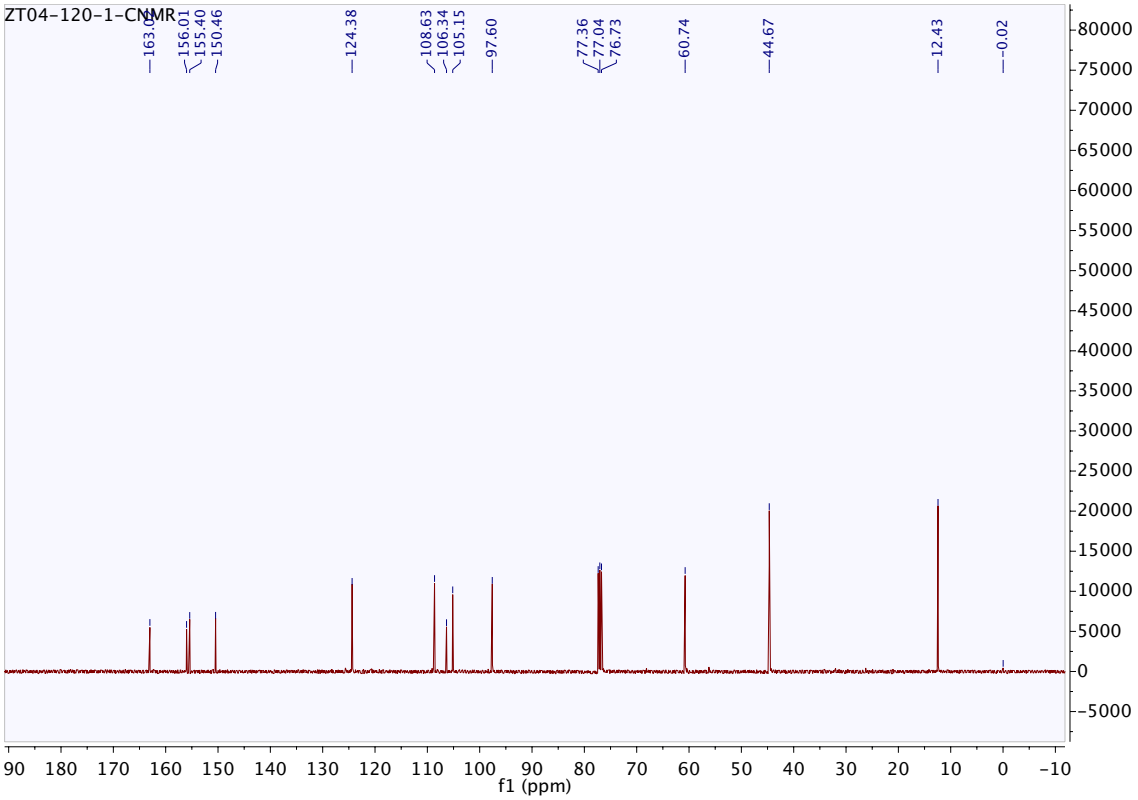

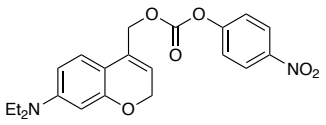

6

^{1}H NMR (400 MHz, $CDCl_3$, 25 °C)

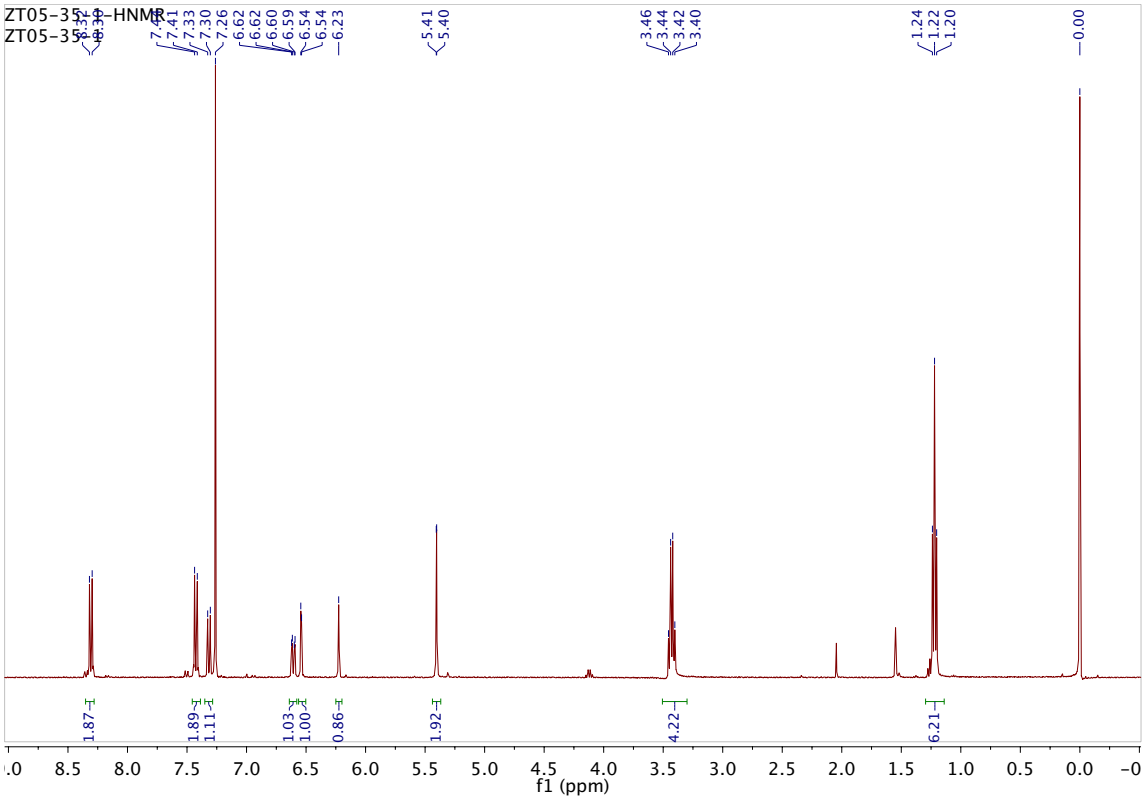

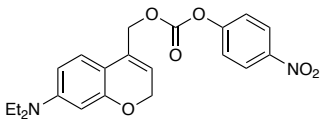

6

^{13}C NMR (101 MHz, $CDCl_3$, 25 °C)

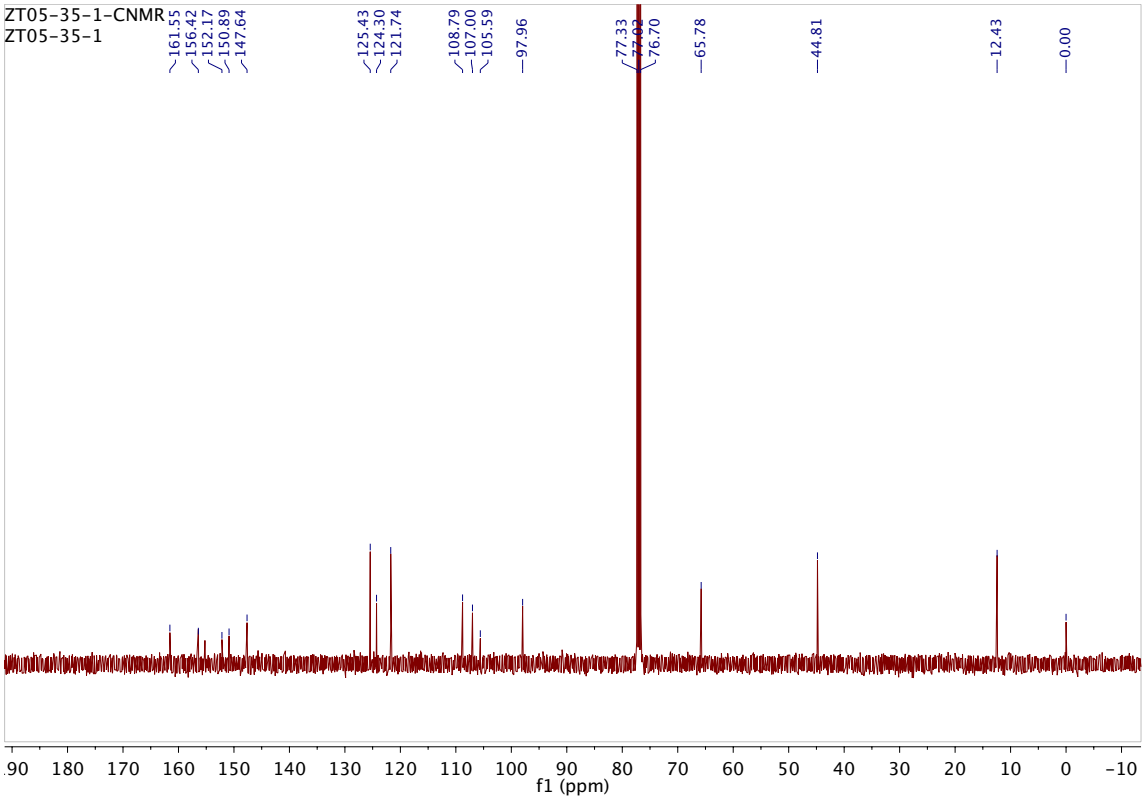

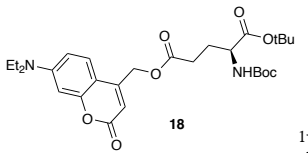

18

^{1}H NMR (400 MHz, $CDCl_3$, 25 °C)

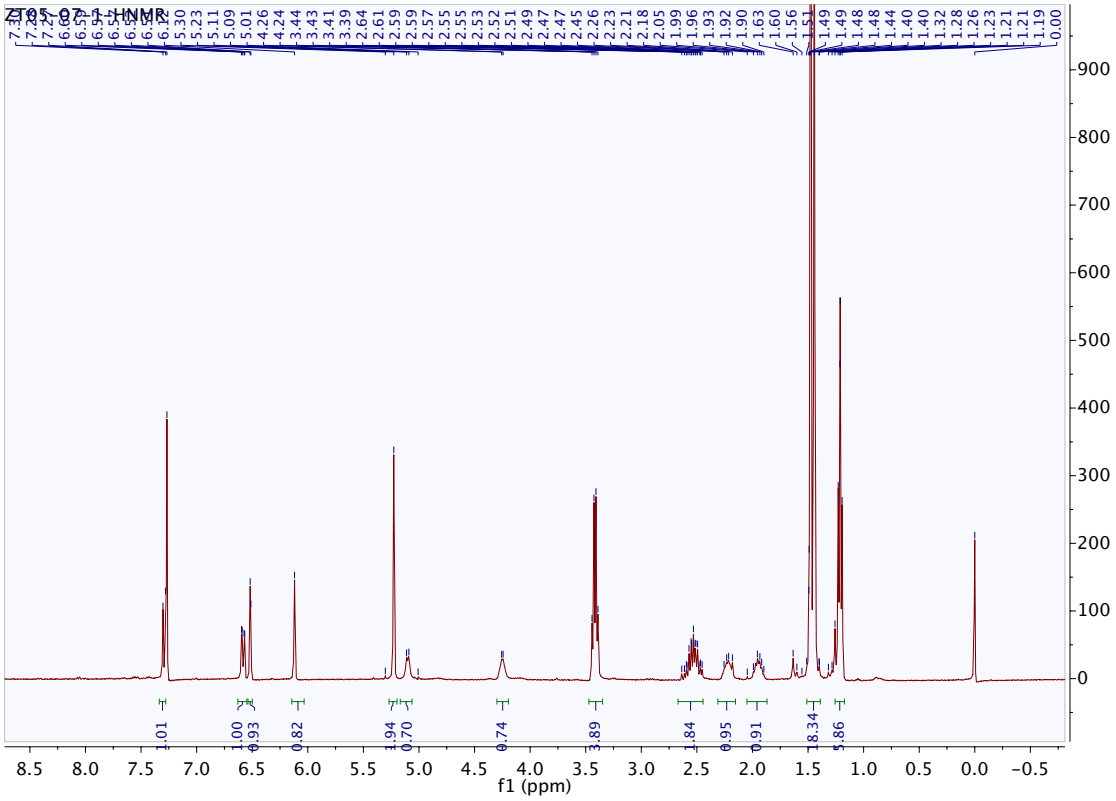

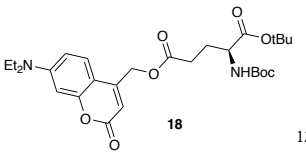

18

^{13}C NMR (101 MHz, $CDCl_3$, 25 °C)

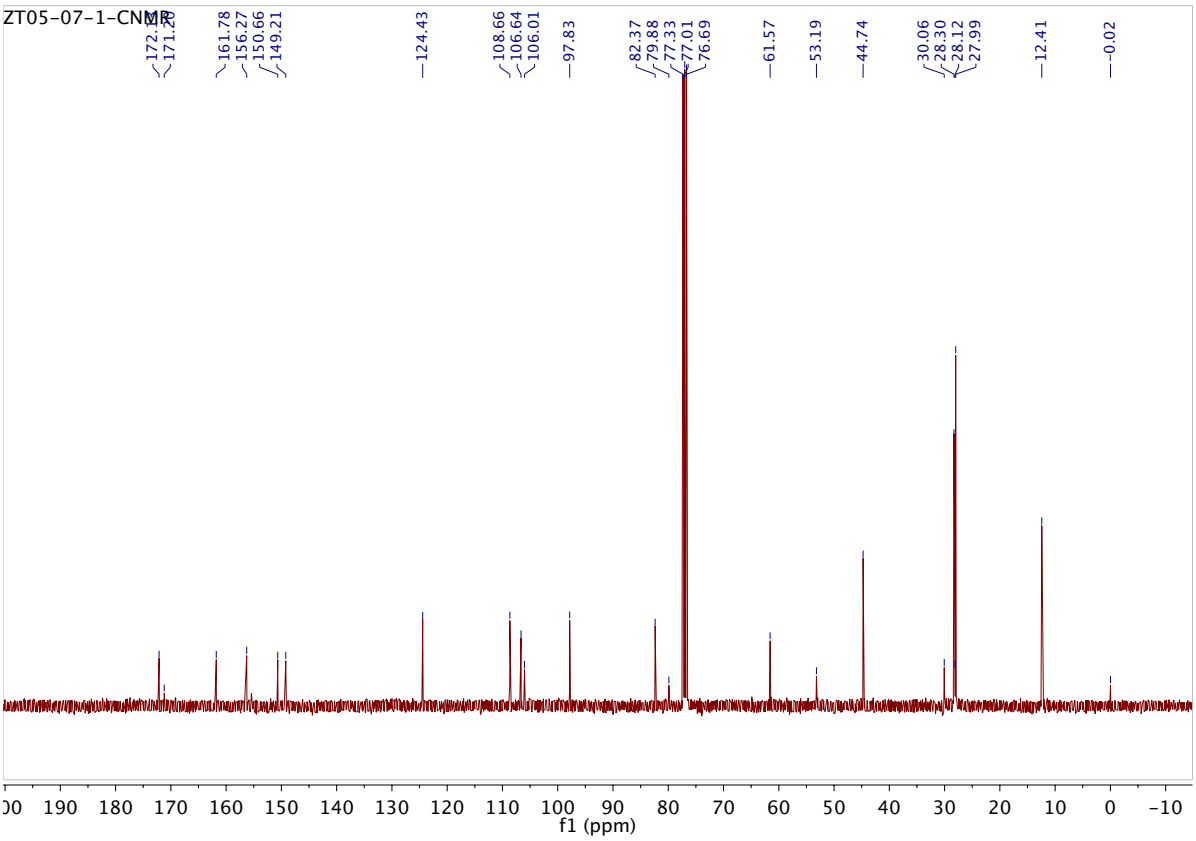

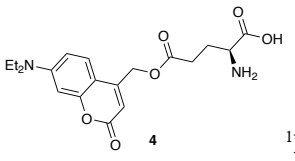

4

^{1}H NMR (400 MHz, CD_3OD, 25 °C)

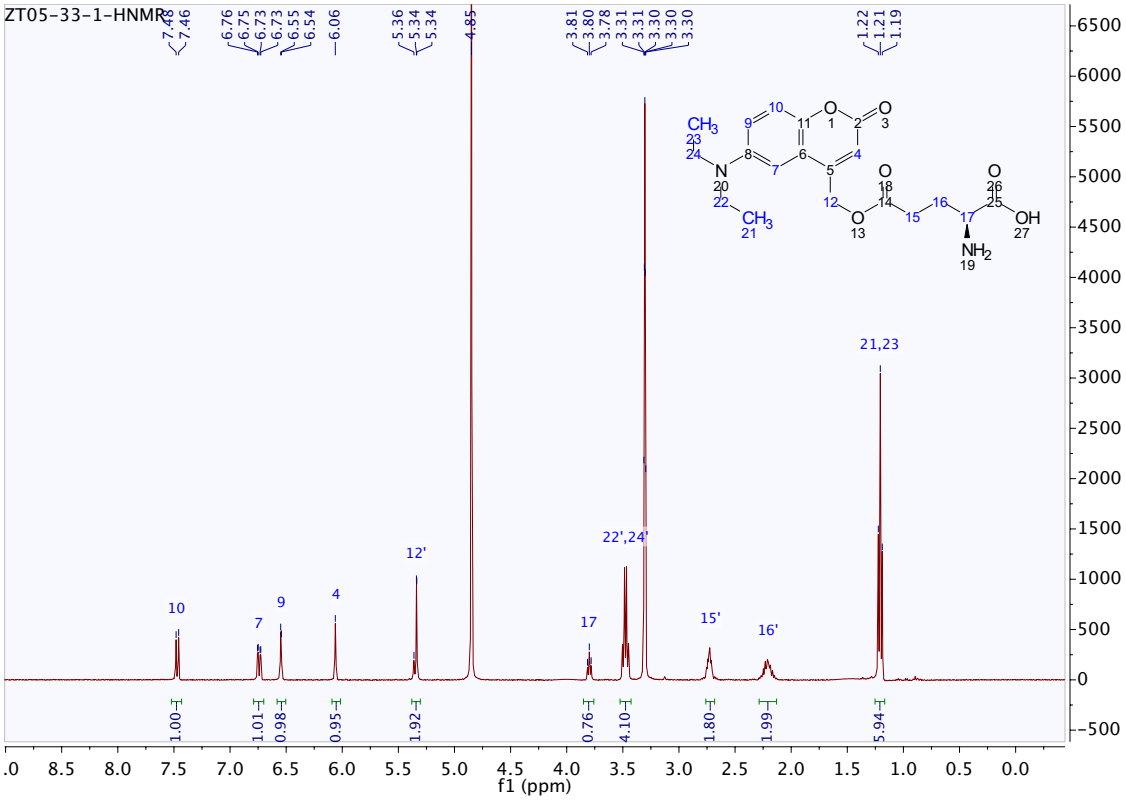

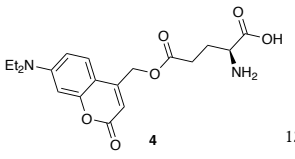

4

^{13}C NMR (101 MHz, CD_3OD, 25 °C)

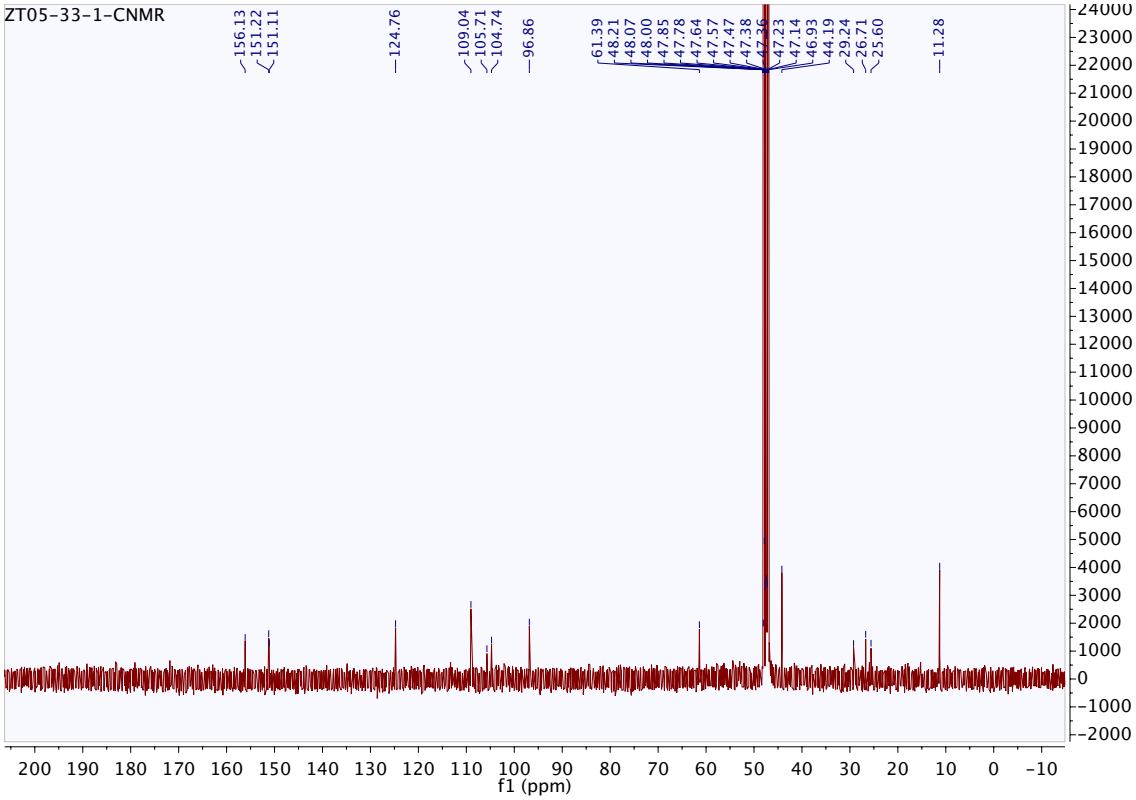

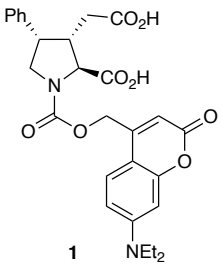

1 ^{1}H NMR (400 MHz, CD_3OD, 25 °C)

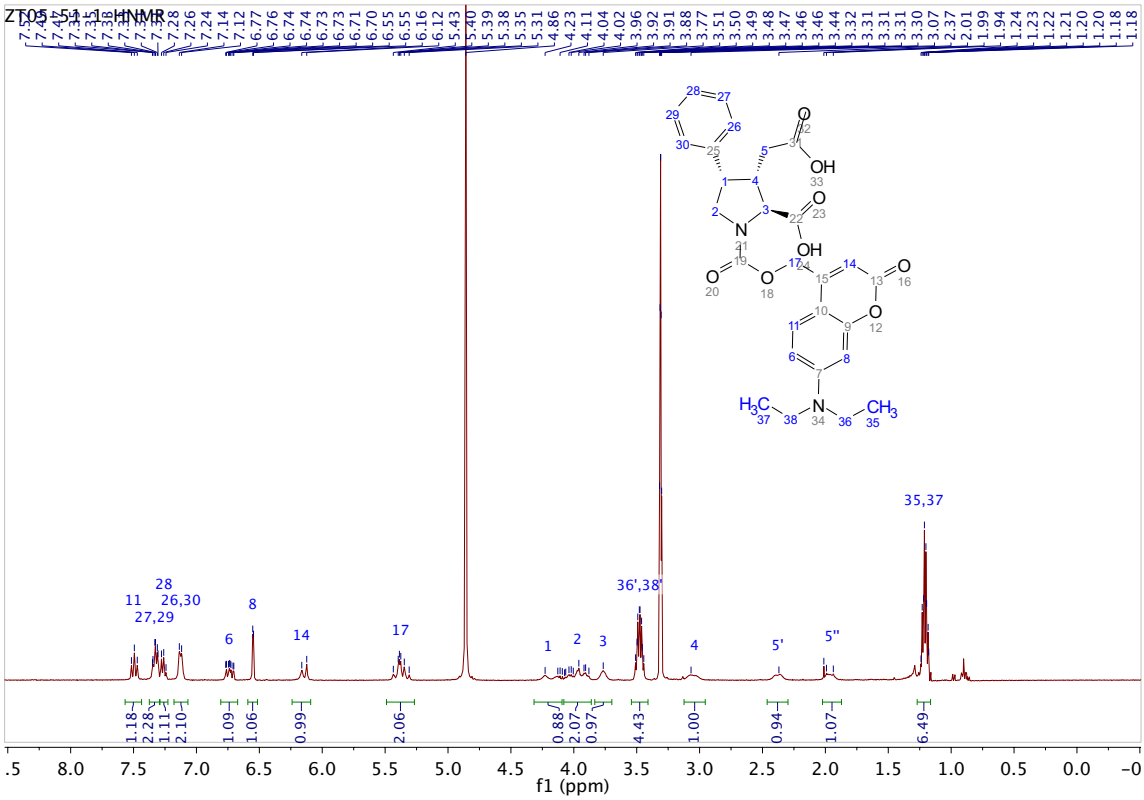

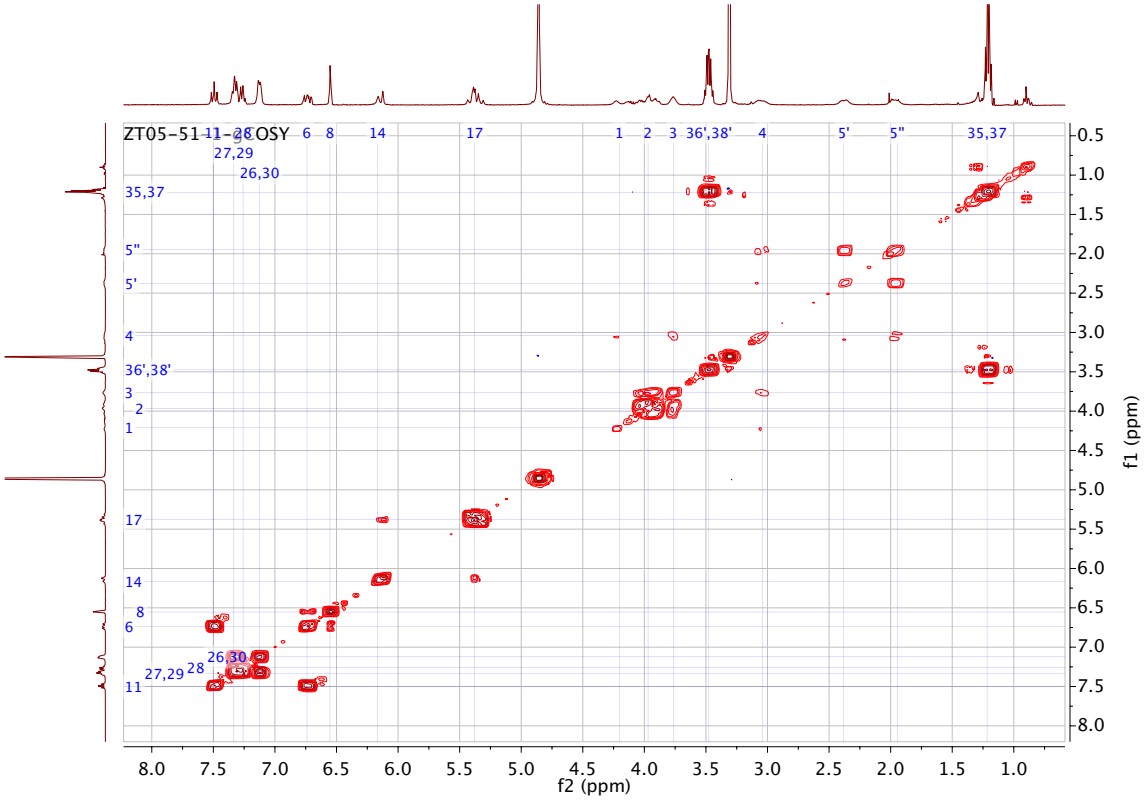
ZT05-51-1-COSY
f2 (ppm)
f1 (ppm)

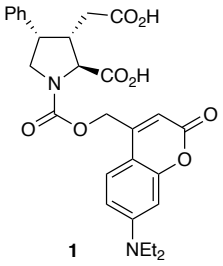

1 ^{13}C NMR (101 MHz, CD_3OD, 25 °C)

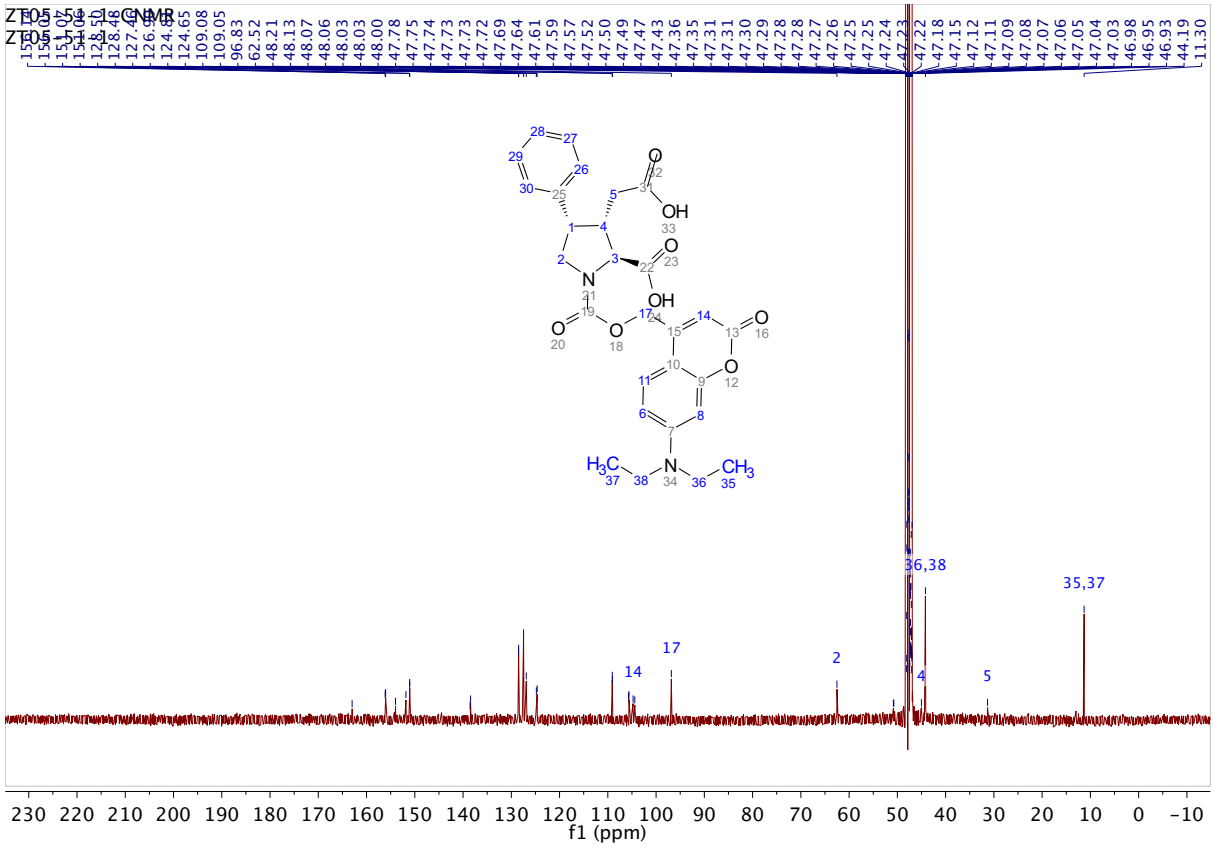

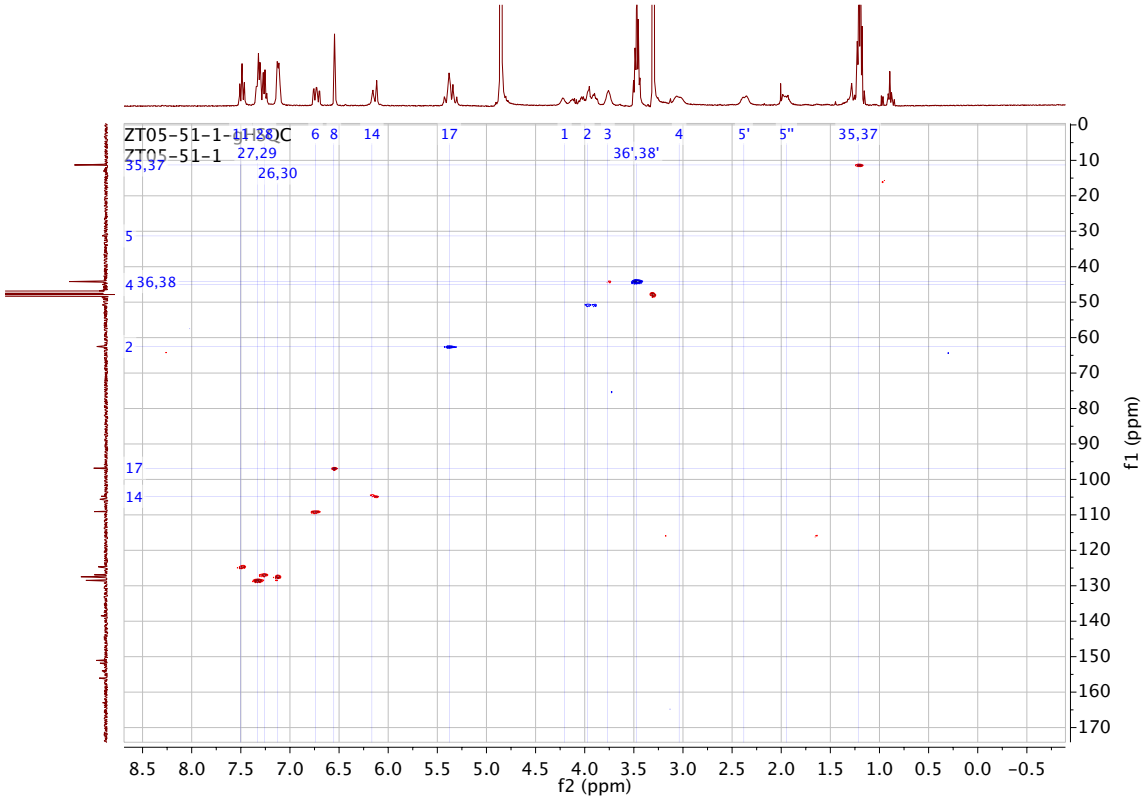
ZT05-51-1-13C
ZT05-51-1
35,37
27,29
26,30
6
8
14
17
1
2
3
36',38'
4
5'
5''
35,37
36,38
5
4
2
17
14
f2 (ppm)
f1 (ppm)